AEROSPACE & DEFENSE™ TECHNOLOGY

The Engineer's Guide to Design & Manufacturing Advances

Welcome to your Digital Edition of *Aerospace & Defense Technology* June 2016

How to Navigate the Magazine:

At the bottom of each page, you will see a navigation bar with the following buttons:

Arrows: Click on the right or left facing arrow to turn the page forward or backward.

Intro **Introduction:** Click on this icon to quickly turn to this page.

Cov **Cover:** Click on this icon to quickly turn to the front cover.

ToC **Table of Contents:** Click on this icon to quickly turn to the table of contents.

Zoom In: Click on this magnifying glass icon to zoom in on the page.

Zoom Out: Click on this magnifying glass icon to zoom out on the page.

Find: Click on this icon to search the document.

You can also use the standard Acrobat Reader tools to navigate through each magazine.

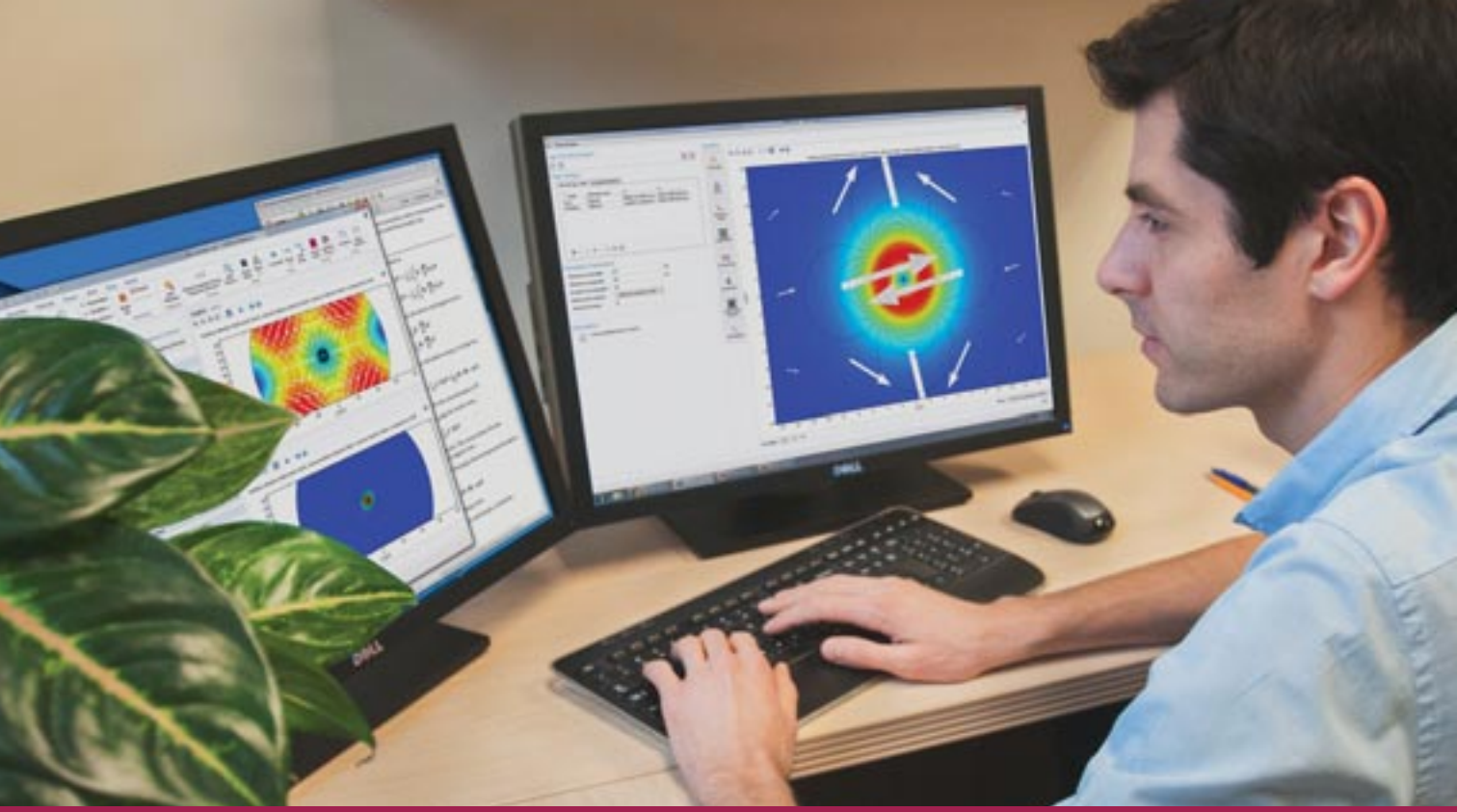

MULTIPHYSICS FOR EVERYONE

The evolution of computational tools for numerical simulation of physics-based systems has reached a major milestone.

Custom applications are now being developed by simulation specialists using the Application Builder in COMSOL Multiphysics®.

With a local installation of COMSOL Server™, applications can be deployed within an entire organization and accessed worldwide.

Make your organization truly benefit from the power of analysis.

comsol.com/application-builder

COMSOL

Free Info at http://info.hotims.com/61062-795

www.aerodefensetech.com

June 2016

AEROSPACE & DEFENSE™ TECHNOLOGY

The Engineer's Guide to Design & Manufacturing Advances

SAE INTERNATIONAL®

Rotorcraft Icing Computational Tool Development

Optical Ice Sensors for UAVs

Designing VME Power Systems with Standard Modules

From the Publishers of TECH BRIEFS

Proven Performance

GORE-FLIGHT™ Microwave Assemblies, 6 Series are ruggedized, lightweight and vapor-sealed airframe assemblies that withstand the challenges of aerospace.

With GORE-FLIGHT™ Microwave Assemblies, 6 Series, a fit-and-forget philosophy is now a reality – providing the most cost-effective solution that ensures mission-critical system performance for military and civil aircraft operators.

Find out why at:
www.gore.com/GORE-FLIGHT

GORE
Creative Technologies Worldwide

Please visit us at Farnborough - 1/B111

precision // lightweight // durability

Follow us on

We are on our way to a much higher standard of manufacturing!

Imagineering is in the process of receiving

AS9100
Certification

from ANAB Accredited Agency

The AS9100 is a technical specification aiming to the development of a quality management system for the Aerospace industry. It provides for continued improvement, emphasizing defect prevention and the reduction of variation and waste.
AS9100 fully incorporates the ISO 9001 standard.

For last 30 years we have been focused on delivering Leading-Edge Technology.Imagineering has been following the highest standards of manufacturing and workmanship in Fabrication & Assembly of Printed Circuit Boards

ITAR Registered ISO Certified UL Approved
WEEE Approved CCR Registered ORCA Registered

30th ANNIVERSARY 1985 - 2015

imagineering inc

Imagineering
Winner of
Family Entrepreneurship
QUINLAN SCHOOL of BUSINESS

Certified Woman Business Enterprise (WBE)
Certified Woman-Owned Small Business(WOSB)
Certification# RWOSB14859 & RWBE14858 (13 C.F.R Part 127)

Free Info at http://info.hotims.com/61062-769

Contents

FEATURES

DEPARTMENTS

ON THE COVER

A CH-47 Chinook helicopter raises a whiteout of blowing snow as it lands in a remote area of Shah Joy district, Zabul province, Afghanistan. Ice forming on the lifting surfaces of a helicopter can cause loss of lift and increase sectional drag forces, negatively impacting performance. Developing tools to accurately model ice buildup on rotors has proven to be challenging. To learn more, read the feature article on page 18.

(Photo courtesy of U.S. Army)

Before "all systems are go," all systems need to be good to go.

Trust Keysight One Source Solutions for all your calibration needs.

When you consolidate all your calibration needs with one trusted partner you'll experience improved performance, increased asset utilization, reduced turnaround time and more success. By supporting Keysight and non-Keysight equipment, no matter how big the problem, or how diverse the test equipment, we'll help you accomplish your mission.

Keysight One Source Solutions	
Supported Calibrations	
Dimensional/Optical	Yes
Electrical	Yes
Electro-Optics	Yes
RF/Microwave	Yes
Physical/Mechanical	Yes

Launch your calibration to the next level.
Get a quote today.
www.keysight.com/find/AmericasOneSource

USA: 800 829 4444 CAN: 877 894 4414

KEYSIGHT TECHNOLOGIES
Unlocking Measurement Insights

Agilent's Electronic Measurement Group is now **Keysight Technologies**.

Free Info at http://info.hotims.com/61062-771

Simulating Thermal Expansion in Composites with Expanded Metal Foil for Lightning Protection

Modern aircraft such as the Boeing 787 Dreamliner are comprised of more than fifty percent carbon fiber composite, requiring the addition of expanded metal foil for lightning strike protection.

The Boeing 787 Dreamliner is comprised of more than fifty percent carbon fiber reinforced plastic (CFRP) due to the material's light weight and exceptional strength. Figure 1 shows the extensive use of composite materials throughout the aircraft. Although CFRP composites inherently have many advantages, they cannot mitigate the potentially damaging electromagnetic effects from a lightning strike. To solve this problem, electrically conductive expanded metal foil (EMF) can be added to the composite structure layup to rapidly dissipate excessive current and heat for lightning protection of CFRP in aircraft.

Engineers at Boeing Research and Technology (BR&T) are using multiphysics simulation and physical measurements to investigate the effect of the EMF design parameters on thermal stress and displacement in each layer of the composite structure layup shown at left in Figure 2. Stress accumulates in the protective coating of the composite structure as a result of thermal cycling due to the typical ground-to-air flight cycle. Over time, the protective coating may crack providing an entrance for moisture and environmental species that can cause corrosion of the EMF, thereby reducing its electrical conductivity and ability to perform its protective function. Through their research, they aim to improve overall thermal stability in the composite structure and therefore reduce the risks and maintenance costs associated with damage to the protective coating.

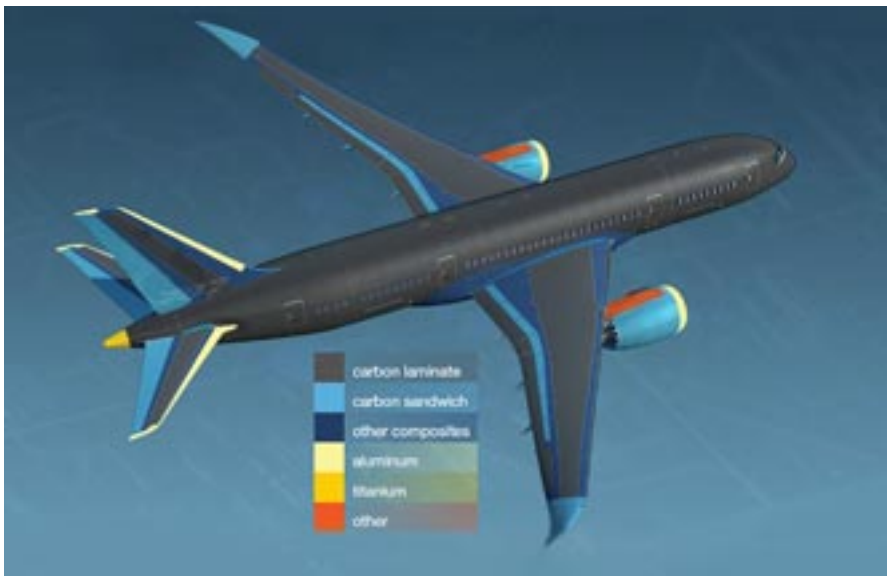

Figure 1. Advanced composites used throughout the Boeing 787 account for more than fifty percent of the aircraft body[1]. (Copyright © Boeing)

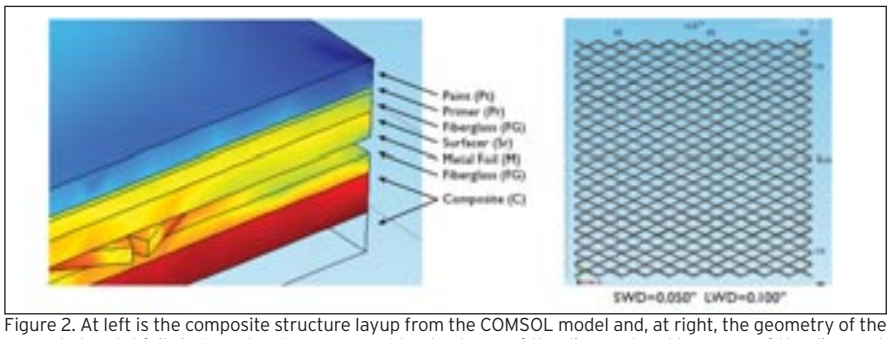

Figure 2. At left is the composite structure layup from the COMSOL model and, at right, the geometry of the expanded metal foil. SWD and LWD correspond to short way of the diamond and long way of the diamond. The mesh aspect ratio: SWD/LWD is one of the parameters varied in the simulations. (Copyright © Boeing)

Simulating Thermal Expansion in Aircraft Composites

In the surface protection scheme shown at left in Figure 2, each layer including the paint, primer, corrosion isolation layer, surfacer, EMF, and the underlying composite structure contribute to the buildup of mechanical stress in the protective coatings over time as they are subject to thermal cycling. The geometry in the figure is from the coefficient of thermal expansion (CTE) model developed by Robert Greegor[2,3] and his colleagues using COMSOL Multiphysics® in order to evaluate the thermal stress and displacement in each layer of a one-inch square sample of the composite structure layup.

The structure of the EMF layer is shown at right in Figure 2. In this study, the EMF height, width of the mesh wire, aspect ratio, metallic composition, and surface layup structure were varied to evaluate their impact on thermal performance throughout the entire structure. The metallic composition of the EMF was either aluminum or copper where an aluminum EMF requires additional fiberglass between the EMF and the composite to prevent galvanic corrosion.

The material properties for each layer including the coefficient of thermal expansion, heat capacity, density, thermal conductivity, Young's modulus, and Poisson's ratio were added to the COMSOL model as custom-defined values and are summarized in Figure 3. The coefficient of thermal expansion of the paint layer is defined by a step function that represents the abrupt change in thermal expansion at the glass transition temperature of the material.

In the CTE model, the Thermal Stress multiphysics interface couples solid mechanics with heat transfer to simulate thermal expansion and solve for the displacement throughout the structure. The simulations were confined to heating of the composite structure layup as experienced upon descent in an aircraft where final and initial temperatures were defined in the model to represent the ground and altitude temperatures, respectively.

Impact of EMF on Stress and Displacement

The results of the COMSOL simulations were analyzed to quantitatively determine the stress and displacement in each layer upon heating and for varied properties of the expanded metal foil. An example of the simulation results is shown in Figure 4.

Through the paint layer at the top of Figure 4, it is possible to observe the displacement pattern of the underlying EMF. The magnified cross-sectional view clearly shows the variations in displacement above the mesh and voids in addition to the trend in stress reduction in the uppermost protective layers. Figure 5 shows the relative stress for each layer in surface protective schemes that incorporate either copper or aluminum EMF. The fiberglass corrosion isolation layer required by the aluminum EMF acts as a buffer, causing the stress to be lower in the aluminum than it is in the copper EMF.

Despite the lower stress in the aluminum EMF, simulation results from the variation of the EMF design parameters reveal a consistent trend toward higher displacements in the surface protective scheme with the aluminum EMF when compared to copper. The larger displacements generally caused by the aluminum EMF can be attributed, in part, to the relatively higher CTE of aluminum.

Further analysis of the impact of the EMF design parameters was performed to confirm the effect of varying the height, width, and mesh aspect ratio on displacement in the protective layers. When varying the mesh aspect ratio, it was found that an increased ratio led to a modest decrease in displacement of about 2 percent for both copper and aluminum EMF, where higher ratio values correspond to a more open mesh structure. For any EMF design parameter, there is a trade-off between current carrying capacity, displacement, and weight. In the case of mesh aspect ratio, while choosing an open mesh structure can reduce displacement and weight, the current carrying capacity that is critical to the protective function of the EMF is reduced as well and needs to be taken into account.

Similarly with regard to the mesh width, varying the width by a factor of three led to a relatively minor increase

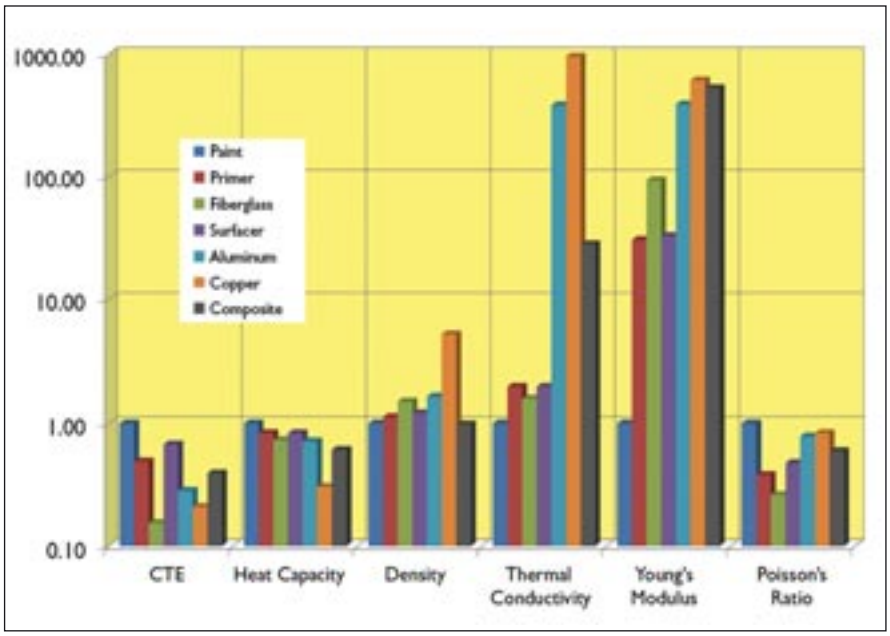

Figure 3. Ratio of each material parameter relative to the paint layer. The paint layer shows higher values of CTE, heat capacity, and Poisson's ratio indicating that it will undergo compressive stress and tensile strain upon heating and cooling. (Copyright © Boeing)

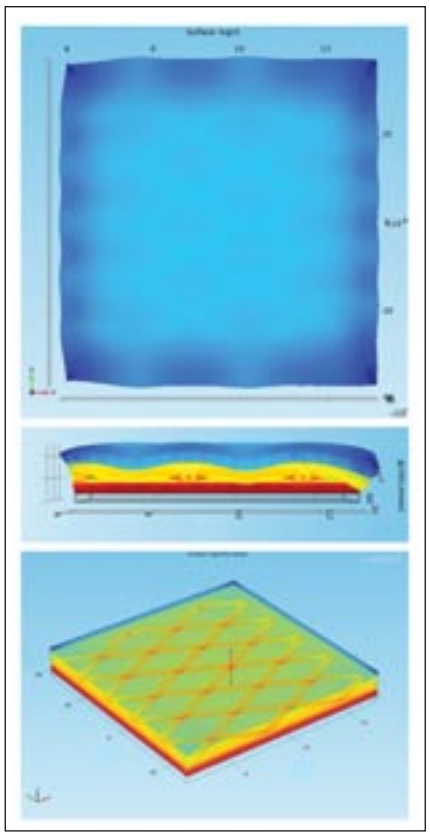

Figure 4. Top & middle: top-down and cross-sectional views of the von Mises stress and displacement in a one-inch square sample of a composite structure layup. At bottom, transparency was used to show the high stress in the composite structure and EMF. Stress was evaluated along the vertical line extending through the depth of the sample. (Copyright © Boeing)

Real. American. Originals.

Onsrud machinery

has been synonymous with cutting edge innovation for more than a century. It's our ingenuity which has helped manufacture goods all over the globe, and no coincidence companies leading the way in their respective industries have sought us out for our high-quality CNC machining products. We want you to

#ExperienceOnsrud.

Quality craftsmanship. The finest materials & tailor-made components. American ingenuity.

36" dia. Blade

5-Axis

F427HR40H2 - Dual Head High Rail

Compound miter cutting capabilities on 8" thick 7000 series aluminum, paired with 5-axis machining - within a 16' x 28' machining envelope.

Larger sizes available.

(See this machine cutting)

C.R. ONSRUD

AMERICAN-MADE CNC MACHINERY

120 Technology Drive Troutman, North Carolina 28166 (704) 508-7000 www.cronsrud.com

Free Info at http://info.hotims.com/61062-773

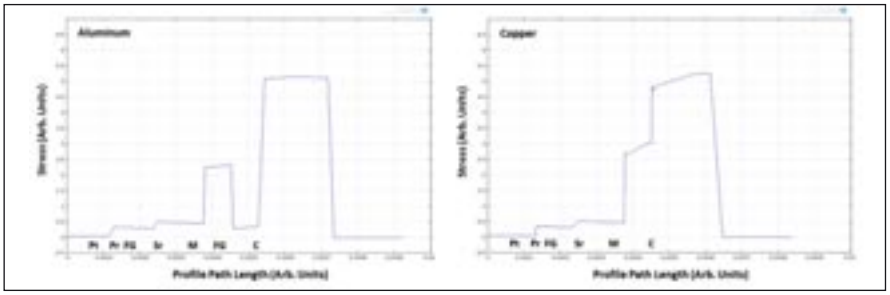

Figure 5. Relative stress in arbitrary units was plotted through the depth of the composite structure layups containing either aluminum (left) or copper EMF (right). (Copyright © Boeing)

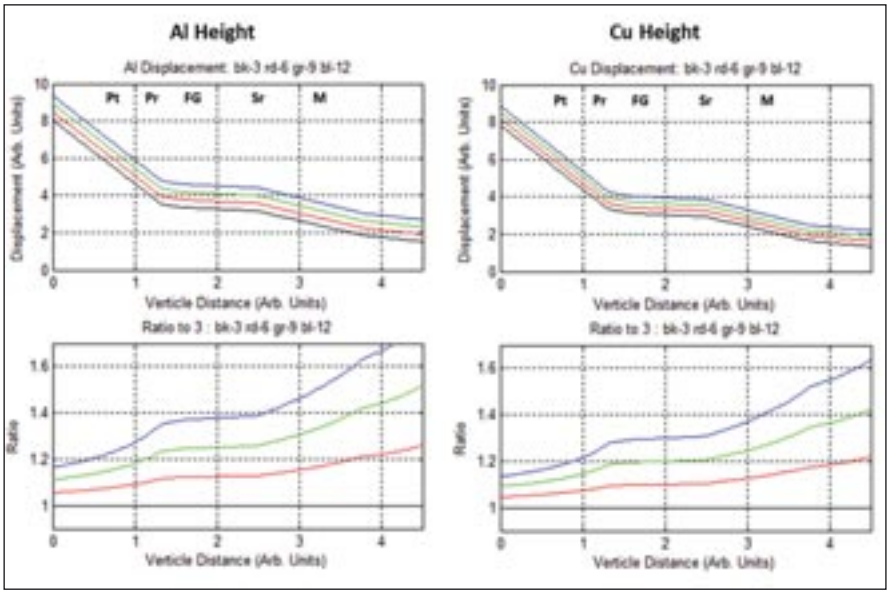

Figure 6. Effect of varying the EMF height on displacement in each layer of the surface protection scheme. The graphs at top show displacement in arbitrary units; at bottom, the ratio is the displacement calculated for each height normalized by the displacement for the smallest height. (Copyright © Boeing)

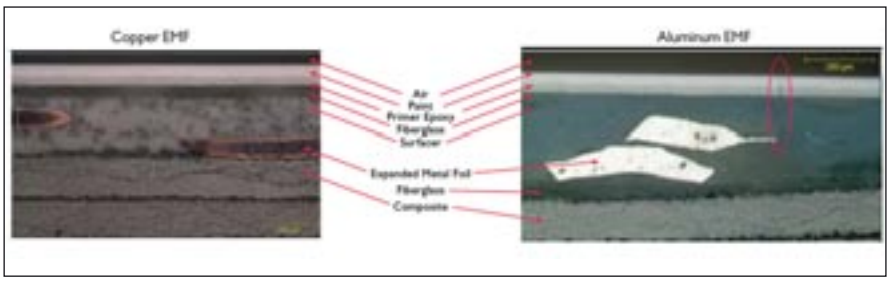

Figure 7. Photo micrographs of the composite structure layups after exposure to moisture and thermal cycling. At left, the results for the copper EMF and at right, the aluminum. (Copyright © Boeing)

in displacement of about 3 percent for both copper and aluminum EMF. However, varying the height of the EMF by a factor of four led to an increase in displacement of approximately 60 percent for both aluminum and copper. Figure 6 shows the relative values for displacement through each layer of the surface protection scheme for varied height of copper and aluminum EMF. Due to the lower impact on displacement, increasing the mesh width or decreasing the aspect ratio are better strategies for increasing the current carrying capacity of the EMF for lightning strike protection.

Relating Displacement with Crack Formation

Greegor and his colleagues at BR&T qualitatively regard any projected increase in displacement as an increased risk for developing cracks in the protective layers since mechanical stress due to thermal cycling accumulates over time.

Experimental evidence supports this logic as shown in Figure 7 in photo micrograph cross-sections of surface protection schemes with aluminum and copper EMF after prolonged exposure to moisture and thermal cycling in an environmental test chamber. The layup with the copper EMF shows no cracks, whereas the aluminum EMF led to cracking in the primer, visible edge and surface cracks, and substantial cracking in mesh overlap regions.

Over the same temperature range, the experimental results correlate well with the results from the simulations that consistently show higher displacements in the protective layers for the aluminum EMF. Both simulation and experiment indicate that the copper EMF is a better choice for lightning strike protection of aircraft composite structures. Multiphysics simulation is therefore a reliable means to evaluate the relative impact of the EMF design parameters on stress and displacement to better understand and reduce the likelihood of crack formation.

This article was written by Jennifer A. Segui, Technical Marketing Engineer, COMSOL (Burlington, MA). For more information, visit ***http://info.hotims.com/61062-502***

References:

The information presented in this article is based on the following publicly available sources:

1. The Boeing Company. 787 Advanced Composite Design. 2008-2013. www.newairplane.com/787/design_highlights/#/visionary-design/composites/advanced-composite-use
2. J.D. Morgan, R.B. Greegor, P.K. Ackerman, Q.N. Le, Thermal Simulation and Testing of Expanded Metal Foils Used for Lightning Protection of Composite Aircraft Structures, SAE Int. J. Aerospace 6(2):371-377, 2013, doi:10.4271/2013-01-2132.
3. R.B. Greegor, J.D. Morgan, Q.N. Le, P.K. Ackerman,Finite Element Modeling and Testing of Expanded Metal Foils Used for Lightning Protection of Composite Aircraft Structures, Proceedings of 2013 ICOLSE Conference; Seattle, WA, September 18-20, 2013.18-20, 2013.

Explore the limits.
T&M solutions for aerospace and defense.

Visit us at
IMS in San Francisco,
booth 1827

Today's aerospace and defense technologies demand ever more sophisticated test and measurement solutions to stretch the limits of what is feasible. As a full-range supplier, Rohde&Schwarz offers a broad portfolio that proves its capabilities in even the most demanding applications. Our leading-edge expertise in microwave, RF and EMC helps customers assess performance, optimize platforms and get the most out of systems. Convince yourself.

www.rohde-schwarz.com/ad/sat/nwa

Technological highlights: network analysis

- Easy-to-use modular solutions up to 500 GHz
- Pulse profile measurements with high resolution
- Precise group delay measurements on frequency converters without LO access
- Absolute phase measurements on mixers

ROHDE&SCHWARZ

Free Info at http://info.hotims.com/61062-774

DESIGNING VME POWER SYSTEMS WITH STANDARD MODULES

Off-the-shelf DC-DC converter and EMI filter modules enable rapid development of custom power solutions.

Military electronics continue to push the performance envelope in all directions. Each new system design faces the same challenges: the need for more processing power, tighter specs, and shorter development time. Continual advances in system performance often require similar advances in the power system. VME architecture is common in many military applications, as systems can readily be built around standard or custom circuit cards. Off-the-shelf VME power supplies are available, but often don't meet the necessary requirements or haven't kept up with recent performance advances. Usually, neither schedule nor budget allow for a full custom power supply development effort.

Fortunately, an optimized VME power supply solution can be built from standard off-the-shelf high-reliability or COTS DC-DC converter modules. This solution can be rapidly developed at minimal cost since most of the design effort is internal to the modules. Input power bus requirements such as MIL-STD-704, MIL-STD-1275, RTCA DO-160 Section 16, and DEF STAN 61-5 can be met by combining standard DC-DC converter, EMI filter, and transient protection modules. Control and telemetry functions, secondary filtering, and other special requirements can be implemented with discrete circuitry. This modular approach can be made to fit almost any application, achieving the same end performance as a custom power supply with much lower risk.

For military, avionics and other high reliability applications it is best to choose DC-DC converters from a manufacturer who focuses on these applications. Look for high quality standards such as J-STD-001 and IPC-A-610 class 3, or for the most critical applications, MIL-PRF-38534 Class H or Class K. Products should have a wide temperature range, -55°C to 100°C or more, a wide input voltage range, and rugged mechanical construction. Additionally, the environmental qualification should be to MIL-STD levels.

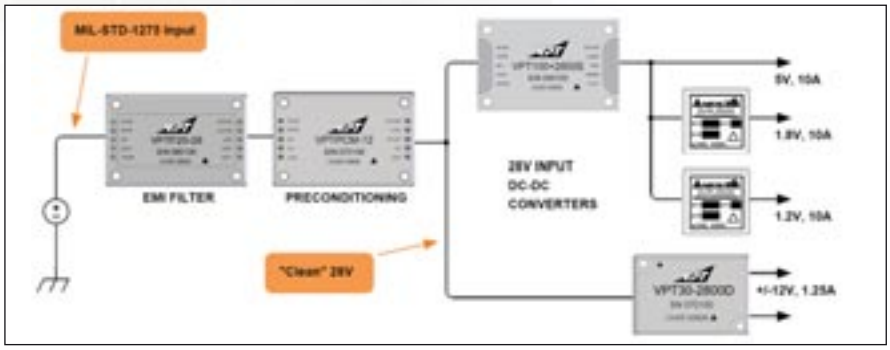

Figure 1. MIL-STD compliant 28V input power supply.

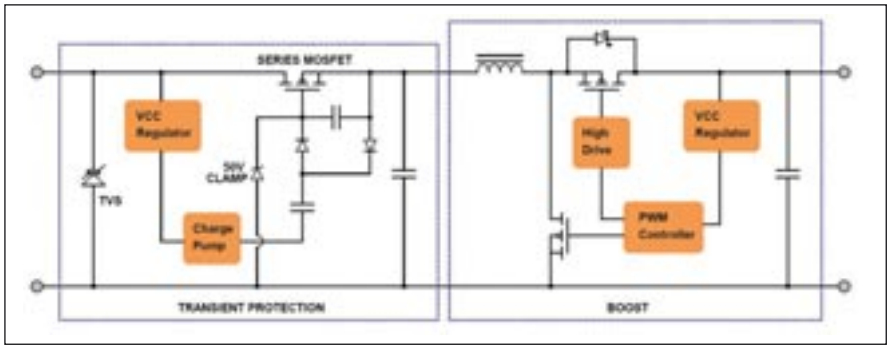

Figure 2. Input Voltage Conditioning Circuit.

28 VDC Input Requirements

The power requirements for most VME applications are defined by a government or commercial standard. For example, equipment for an aircraft application might have to meet MIL-STD-704 or RTCA DO-160, while a vehicle application might need to meet MIL-STD-1275. These documents specify steady state voltage ranges, but also voltage ripple, abnormal conditions, and undervoltage and overvoltage transients. An EMI requirement such

Critical Moments call for Critical Products

Coilcraft CPS has the battle-proven magnetics you need when the mission is on the line

Our critical-grade RF and Power inductors are built to withstand the most punishing conditions imaginable, including extreme temperatures, thermal shock, G-forces, EMI and vibration.

- Tin-lead (Sn-Pb) terminations for the best possible board adhesion. RoHS terminations also available.
- Extended temperature ranges (-55°C to +200°C)
- Vibration testing to 80 G / shock testing to 1000 G

We also offer comprehensive product testing and validation services in accordance with MIL-STD-981 and EEE-INST-002, as well as custom screening to your electrical and physical specifications.

Learn more about how our battle-tested components will keep your mission on target. Call or visit us online today!

Coilcraft CPS
CRITICAL PRODUCTS & SERVICES

800.981.0363 847.639.6400 www.coilcraft-cps.com

Free Info at http://info.hotims.com/61062-775

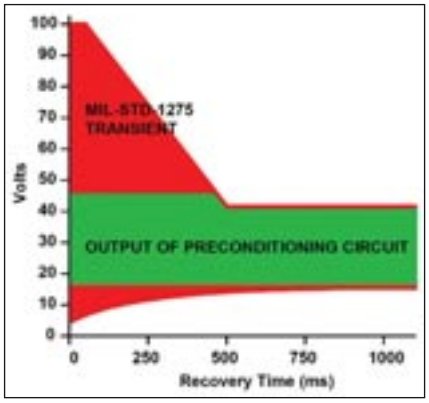

Figure 3. MIL-STD-1275 transients.

as MIL-STD-461 governing the conducted emissions and conducted susceptibility will also need to be met. Many DC-DC converters are available for the 28 VDC power bus, but assembling a robust system design which meets every requirement can still be complex. A typical compliant design includes several DC-DC converters, an EMI filter, and possibly a preconditioning or transient protection module as shown in Figure 1.

In the various standards governing input power bus conditions, there are several areas which cause headaches for power designers. MIL-STD-704 revision A includes an 80V transient, a minimum steady state voltage of 15V, and up to 2V peak of ripple on the input; while in later revisions, the transient is 50V, the minimum steady state voltage is 16V, and the ripple is 1.5V peak. DO-160 includes transients up to 80V, transients down to 17V, and ripple up to 2V peak. Some systems may be required to operate through an engine starting condition where the input can drop as low as 10V or 12V, and others might be further required to operate through a momentary loss of input.

Compliance starts with the DC-DC converter. Its input voltage range should be as wide as possible to cover the input power bus conditions. Typical DC-DC converter input voltage ranges are 16V to 40V, 15V to 50V, or 9V to 60V with transient capability of 50V, 80V or 100V. If the DC-DC converter does not meet the full input requirement standalone, additional circuitry can be used to achieve compliance.

Input Voltage Conditioning Techniques

The two-stage input voltage conditioning circuit shown in Figure 2 accommodates input transients that extend both above and below the operating range of the DC-DC converter. The first stage performs the overvoltage protection function while the second stage boosts low input voltages into range.

The overvoltage transient protection activates when the input voltage exceeds the input range of the DC-DC converter. Short duration, high voltage spikes are first clamped with a transient voltage suppressor device. Longer duration transients, such as the 80V surge in MIL-STD-704A or in DO-160 or the 100V surge in MIL-STD-1275, must be limited with a series device. As illustrated in the figure, this is accomplished with a series pass MOSFET, operated in its linear mode. An N-channel MOSFET is chosen for low on-resistance and high power handling capability. Care should be taken to ensure the MOSFET stays within its safe operating area, as it dissipates high instantaneous power, dropping 50V while passing several amps. A charge pump drives the gate voltage above the input, turning the MOSFET "on" fully for low power loss during normal operation. A Zener clamp on the gate forces the MOSFET to act as a source-follower, or effectively a series pass linear regulator, during an input voltage transient. The output is then safely limited to less than 50V.

The "boost" portion of the input voltage conditioning circuit is necessary when operation is required for input voltages below the range of the DC-DC converter. Typical such scenarios include operating through the 6V "initial engagement surge" of MIL-STD-1275 or during engine starting in MIL-STD-704 and DO-160. If continuous operation is not required, the DC-DC converter can be allowed to naturally turn off and back on. A synchronous boost topology is utilized, with the output diode replaced by a MOSFET, for lower losses and increased efficiency. During normal operation, the boost remains off, and the high-side MOSFET fully on. This requires a high side drive with 100% duty cycle capability, typically implemented with a charge pump and level shifter for the gate signal. As the input voltage drops, the boost must respond, turning on very quickly, otherwise a dip on its output could cause the downstream DC-DC converter to glitch or turn off momentarily. This requires a fast control loop with a fast mode transition.

Figure 3 gives a worst case envelope of the input voltage transients from MIL-STD-1275D along with the output envelope of the preconditioning circuit. Voltages above the range of the DC-DC converter are limited by the series pass MOSFET, while inputs below the input range are boosted. The resulting output is controlled within the operating range of the DC-DC converter.

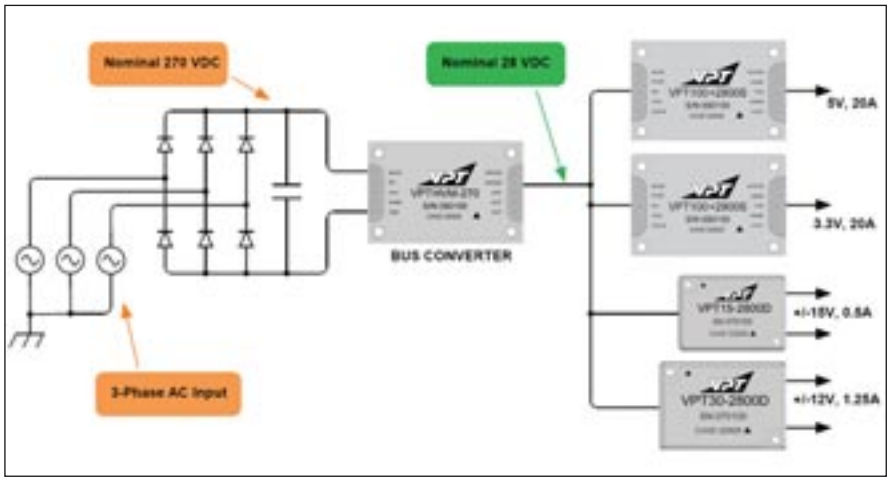

Figure 4. AC input power supply constructed with 28V input DC-DC converters.

Accommodating Higher Voltage and AC Inputs

High voltage power buses, such as 270 VDC or 115 VAC can be accommodated in several ways. At the card or box level, it's advantageous to first perform a bulk conversion to 28 VDC, then use individual converters to regulate the different low power outputs. This approach works with both DC and AC inputs, and can often result in a simpler overall design, as it not only minimizes the amount of high voltage wiring, but also takes advantage of the variety of 28V input products available.

A typical aircraft power system design is shown in Figure 4. The input shown is a 3-phase wye connected grounded-neutral system typical of MIL-STD-704 with a nominal voltage of 115V AC and a nominal frequency of 400 Hz. A 3-phase six-diode rectifier and bulk capacitor is used to convert the 3-phase AC to a nominal 270 VDC. A bus converter is used to convert the 270 VDC into a 28V power bus which can then be converted to various lower voltages with standard 28V input DC-DC converters.

The Final Assembly

With proper system design, standard 28V input DC-DC converters can satisfy a variety of input power bus requirements. The DC-DC converters, EMI filters and accessory modules are readily mounted to a PCB and packaged in a conduction or convection cooled housing. Power modules with a temperature rating of -55°C to +100°C can easily meet a final power supply specification of -55°C to +85°C rail temperature. Additional discrete circuitry can be added for enable signals, input and output monitoring, over temperature protection, status LEDs, and even output sequencing and timing. The input and outputs can also be tweaked with additional filtering for ultra-low ripple or with post linear regulators.

Figure 5. VME power supply built from off-the-shelf DC-DC converter modules.

The VPTVME-28, shown in Figure 5, is a highly configurable VME power supply built from VPT Series COTS modules. The output voltages and power levels, as well as the number of outputs and I/O signals, are configurable for almost any application.

This article was written by Steve Butler, Director of Advanced Product Development, VPT, Inc., (Blacksburg, VA). For more information, visit ***http://info.hotims.com/61062-500****.*

Optical Ice Sensors for UAVs

Vibrating-reed ice detectors from the 1980s are designed for controlling inflatable rubber boots, but today's UAVs require a more modern approach.

The perverse thing about ice on the tailplane of a general aviation aircraft is that the pilot sits and looks forward, but the tailplane is aft. You can't see it from the cockpit.

One sign there's ice on the tailplane of a general aviation (GA) aircraft in flight is when the controls become "mushy". That's a tactile clue, but when there's no human being with hands on the controls, it's a compound problem for unmanned aerial vehicles.

As for ice on the wings etc., GA pilots are trained to "look for ice". Again, without a human being in direct control, it's a double problem for UAVs. But even so, how do you see clear ice? How do you see white ice on a white wing? How do you see ice at night?

Clearly, ice sensors are de rigueur for UAVs.

UAVs can fly at great heights, and for long periods of time. But in order to get up there, they have to transit through the hazardous ice-formation zone below 20,000 feet; that's where ice forms. Above that altitude, it's generally too cold for ice to form on the airframe. Because the temperature lapse rate of our atmosphere is -3.5 deg F per 1000 feet, H_2O molecules in the air up there may already be in their solid phase, and they just bounce off.

It's when liquid water molecules (clouds) impinge on the airframe and freeze in place – that's the danger.

Ice forms on thicker members of an airframe later (windshields and wings). That's because thicker cross-sectional members compress more H_2O molecules, and their cumulative ram-air heating effect is greater than it is on thinner cross-sectional members (horizontal stabilizers and rudders of the tailplane empennage). Less compressional heating means the tailplane remains colder, and ices up earlier, before the wings do.

So, the perversity of ice on an aircraft tailplane is that ice is more likely to form there than on the wings; the tailplane can't be seen, and the deleterious effects of ice on the horizontal stabilizer can be greater than ice on the wings, especially on landing.

Wing ice on the leading edges and upper surfaces is bad enough. It destroys lift, and the weight of it (90% that of water) not only burdens the powerplant, but is mostly forward of the center of gravity, inducing the nose to point down, toward the ground.

On landing, the effect of ice on the horizontal stabilizer is definitely worse than on the wing. An aircraft's horizontal stabilizer is actually a small wing, mounted upside-down. It creates downward "lift", forcing the tail down, and the nose up. If the horizontal stabilizer stalls on landing, the nose can pitch down very abruptly and violently. Ice-induced tailplane stall on landing is really bad, because there may not be enough altitude remaining in which to recover.

In-flight situational awareness is even more critical in a UAV than in a manned aircraft because of the absence of tactile feedback to a human pilot.

Bristling With GPS and Other Gear

Most large air transport and military aircraft are normally equipped with pneumatic de-icing boots made of rubber. These boots have been around since

Figure 1. This commercial, off-the-shelf, in-flight ice sensor monitors the optical characteristics of whatever substance is in contact with the optical surfaces of the probe, either air (NO ICE) or water ice (ICE ALERT). Ambient wind blows standing water away, but ice sticks. Made of nonconductive delrin and acrylic plastics, probe is electromagnetically compatible with its host aircraft radio environment, and can be installed in close proximity to radio antennas.

the 1940s and earlier; they can be activated manually by the pilot, or automatically, by an on-board ice sensor.

Since the advent of rubber boots, more recent developments for aircraft de-icing include hot bleed air from the engine's exhaust, electrical heaters, ethylene glycol weeping wings, capacitive discharge loops that literally blast ice off the leading edges, and others. Historically by default, most automatic de-icing schemes use ice-sensing technology based on a vibrating reed, from the 1980s.

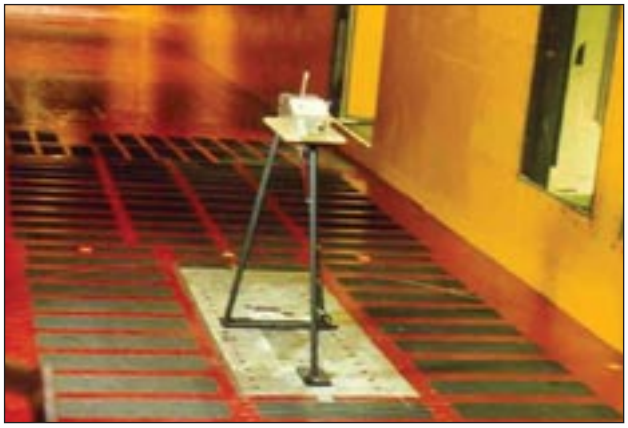

Figure 2. Test program conducted at NASA Glenn's Icing Research Tunnel demonstrates sensor conformity with defacto standard SAE AS 5498 ¶5.2.1.1.1 minimum operational performance for in-flight icing detection systems. Also listed in SAE AIR 4367 ¶ 4.11. (Note NASA Pitot tube in left foreground, rotating deck for adjusting wind tunnel icing angle-of-attack).

Vibrating-reed ice sensors protrude from the fuselage of an aircraft into the ambient airstream and resonate in free air at 40 KHz. When ice forms on the probe, its mass reduces the frequency of vibration. The sensor housing contains a circuit board that translates that change in frequency to an equivalent mass on the probe. Then another circuit board translates that equivalent mass to a theoretical thickness of ice, which, if it exceeds a threshold of typically 0.020 inch, the unit reports ice alert. This signal then activates pneumatic boots which expand and crack the ice away from the wing's leading edge.

Even for aircraft that do not employ pneumatic de-icing boots, vibrating ice detectors have been the default ice sensors for 30 years, providing advisory ice alerts to pilots, advising them to take some corrective action – climb up out of the clouds to clean air, descend below the clouds to warmer air, or turn around and go back. All this is well and good, but when it comes to modern unmanned aerial vehicles, mechanically vibrating ice sensors are less than an optimum solution. In a major break-

through in ice sensor technology development, today's newest and most up-to-date ice sensors are available on the open market for subsonic aircraft.

Optical ice sensors are especially suitable to UAVs because they are small, lightweight, sensitive, and their probes can be made entirely of nonconductive plastic.

Modern UAVs are used as airborne platforms for surveillance, mapping, communications, fire fighting, agriculture, search & rescue, and other radio-intense applications. Compared with traditional general aviation aircraft, modern UAVs tend to be smaller and lighter, with less powerful engines, a lower energy budget, and bristling with GPS and other radio gear.

H_2O Phase Change

Just as any other radio antennas, transmitting and receiving antennas on UAVs require a sphere of elbow room in which to propagate and receive electromagnetic signals correctly, without interference from nearby electrically-conductive structures that might distort and corrupt their frail, low-level satellite and terrestrial radio signals.

The limited surface area for ice sensor probes on a small UAV can complicate the location and installation of any kind of metal ice sensor vis-a-vis the aircraft's sensitive radio antennas. Solving this problem, the external sensing probe of modern aviation ice sensors is fabricated of non-conductive plastic that is transparent to radio signals, and poses no radio interference problem for the host UAV.

Modern optical ice sensors generally consist of a unitized plastic probe with an air gap, circuit board, housing, and cable. The probe is a delrin plastic cantilever that holds two optical windows and a reflecting wall below the wing, out into the airstream. In operation, optical ice sensors detect the H_2O phase-change between liquid water and solid ice. Producing the maximum possible sensitivity, in-flight ice molecules form directly on the probe's optical surfaces.

Figure 3. Simple field test procedure sprays tetrafluoroethane component cooler on air gap optical surfaces, freezes ice out of ambient moisture, and tests rate-of- accumulation: ICE ALERT, MORE ICE, SATURATION.

Cov ToC

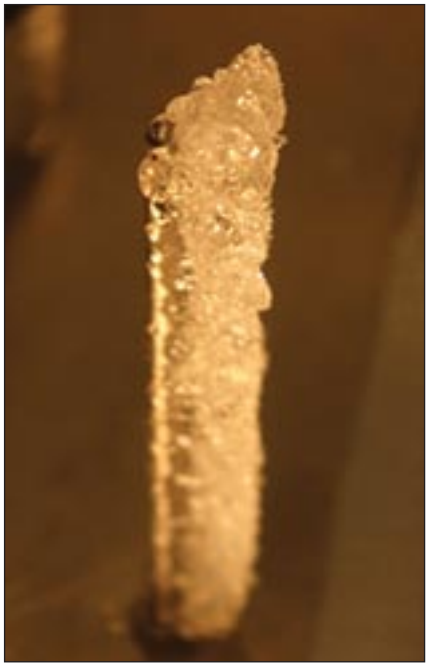

Figure 4. Saturation ice on a modern optical ice sensor probe.

For more information on ice-induced tailplane stall, interested readers may wish to view a 23-minute NASA video entitled "TAILPLANE ICING" that excellently describes, illustrates and dramatizes the hazards of ice-induced tailplane stall, and its effects on aircraft safety while landing. For information, contact NASA Glenn at email grc-icing@lists.nasa.gov, or visit ***http://icebox.grc.nasa.gov/education/products.html***. Also, a limited number of digital video disks are available directly from the author, email RLH@newavionics.com

An optical sensor-excitation signal is created and received by the interface board. The earliest formation of ice molecules on the optical surfaces perturbs the sensor's excitation signal, on a molecular level. The board interprets and outputs transducer signal variations on three discrete logic wires as no ice (000), ice alert (001), more ice (011), or saturation ice (111). The probe's inboard end mates with a small interface board buried in solid epoxy inside the housing, completely submersible in water. A lightweight blue cable connects the unit to its host system.

Optical ice sensors are small, lightweight, have no MHz clock, and no moving parts. They install from inside the wing, extending down, air gap facing forward into the air stream. The entire unit is fixed in place with a 5/16"-24 thread and nut, just as an ordinary outside air temperature gauge installs in a general aviation aircraft.

Optical ice sensors owe their high degree of sensitivity to the fact that they are pencil thin, and so create minimum ram-air heating effect on airborne H_2O molecules. For this reason, they attract solid ice molecules before fatter, warmer airframe members, such as fuselage, wings and struts. During NO-ICE conditions, ambient wind removes liquid water from the sensor optics, but ice sticks to it and accumulates for detection.

NASA Glenn's Icing Research Tunnel, the world's largest such tunnel in Cleveland Ohio, has tested and documented optical ice sensors according to a matrix of temperature, humidity, altitude, air speed, liquid water content, drizzle drop diameter, and air pressure. Test tunnel matrix and report available upon request.

Shape-Changer

Ice formations on an exposed optical surface in an icing domain can be either clear ice or rime ice, depending upon atmospheric variables. But optically clear ice or opaque rime ice makes no difference to the sensor. Optical ice sensors can change their shape according to the type of ice formation and report it. When shipped from the factory, optical ice sensors have one shape, but when installed in a UAV, flown aloft and faced with ice, they can change to a different shape. Because they are completely solid and lightweight vs vibrating sensors, optical ice sensors are extremely robust vs shock and vibration. They create less aerodynamic drag than vibrating sensors, and they add lightness to any aircraft. One of the reasons for their lightness is they eliminate the weight of many-turns-of-fine-wire magnetic coils required for an electro-magnetically driven sensor probe.

Not only is the weight of the copper eliminated, but also the weight of the metal frame to contain and mount the vibrating assembly. Optical ice sensors employ very simple direct-sensing technology, have no moving parts, and are simple to manufacture and test. Manufacturing cost is much lower than vibrating sensors. What's more, optical ice sensors substantially reduce the power budget of any aircraft. Simple to design into any UAV, they operate on just one single DC voltage anywhere between six and 30 volts. At standard 24 VDC input, they draw less than 100 mA; you can power it with a 5 Watt solar panel. Output logic levels for the three dedicated wires is zero volts to 3.3 volts DC.

Absence of installation-template restrictions affords optical sensors a great deal of flexibility. Probes can be separated from their electronic interface boards, and conveniently integrated directly with UAV running lights and Pitot tubes. Because they are potted solid with two-part epoxy, they are explosion-proof. Because system integration is so simple, sensors are shipped with their connecting wires simply stripped-and-tinned at the end. No requirement for MIL-SPEC connectors.

Modern ice sensors are offered as commercial off-the-shelf (COTS) products. Because of an unfortunate absence of any published FAA TSO specification for in-flight ice-sensors, the aviation community relies upon defacto standard SAE aerospace specification AS-5498, core paragraph ¶5.2.1.1.1. Optical sensors are also listed in SAE aerospace information report AIR-4367 paragraph ¶ 4.11.

As unmanned aerial vehicles become more and more popular throughout the aviation community, modern ice sensors are becoming equally important to help operators of the aircraft avoid the hazards of ice-induced tailplane stall and other ice-related hazards. The recent advent of modern optical ice sensors to supplant primitive vibrating sensors promises to aid the state of the art.

This article was written by Richard Hackmeister, Vice President, New Avionics Corp., (Fort Lauderdale, FL). For more information, visit ***http://info.hotims.com/61062-501.***

Rotorcraft Icing Computational Tool Development

(Photo Courtesy U.S. Army)

The formation of ice over lifting surfaces can affect aerodynamic performance. In the case of helicopters, this loss in lift and the increase in sectional drag forces will have a dramatic effect on vehicle performance. The simulation of rotorcraft flow fields is a challenging multidisciplinary problem that lags in development over its counterpart in the fixed wing world by more than a decade. Successful aerodynamic simulation of a rotor/fuselage system requires the modeling of unsteady three-dimensional flows that include transonic shocks, dynamic stall with boundary layer separation, vortical wakes, blade/wake and wake/wake interactions, rigid body motion, blade deformations and the loss of performance caused by ice accretion.

Stand-alone ice accretion prediction tools, as well as ice accretion fully integrated with aerodynamics, currently exist for 2D airfoils and 3D aircraft configurations. Ice accretion predictions are typically two-dimensional in nature and based on the classical Messinger model. The analysis consists of four critical steps: flowfield calculation, water droplet impingement calculation, heat transfer prediction, and ice accumulation normal to the surface.

LEWICE and LEWICE3D

LEWICE is NASA's flagship code for 2D ice accretion prediction, and it is the core of the 3D ice accretion tools as well. LEWICE development was initiated in the early 1980s, with the first general release (Version 1.0) in 1991. Four major updates to the code followed, in 1993 (Version 1.3), 1995 (Version 1.6), 1999 (Version 2.0) and 2002 (Version 2.2). Recent updates were released in 2005 (Version 3.0) and 2006 (Version 3.2), and a mixed-phase modeling capability was added in 2008.

The code uses a potential panel method to determine the flow field about a clean surface, then calculates water droplet trajectories from some upstream location until they impact the surface or until the body is bypassed. Collection efficiency is then determined from the water droplet impact location pattern between the impingement limits. A quasi-steady analysis of the control volume mass and energy balance is performed next using a time-stepping routine. Density correlations are used to convert ice growth mass into volume. LEWICE also features multiple drop size distributions, multiple airfoil elements, thermal models for anti-icing/de-icing systems, and an interface with structured grid codes, allowing the use of viscous Navier-Stokes flow solutions.

The thermal models in LEWICE combine the features of previous codes, LEWICE/Thermal and ANTICE, to simulate de-icing and anti-icing with electrothermal or hot air systems. Features are included to allow determination of optimized heater sequencing (for electrothermal analysis) and multiple boundary conditions (for bleed air analysis).

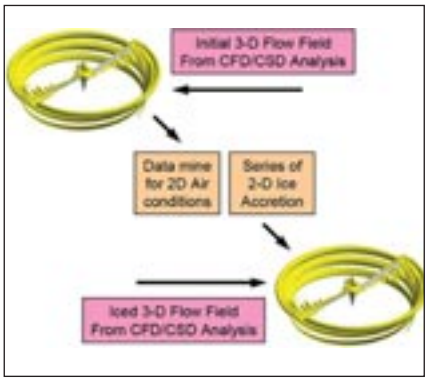

Figure 1. Methodology for Developing a 3D Ice Shape.

LEWICE has been thoroughly validated for a wide range of conditions, with a database of over 3,000 ice shapes on 9 different geometries. Validation has been documented in numerous papers as well as NASA reports. The validation database lies mostly within the Appendix C continuous maximum or intermittent maximum envelopes, but there are some exceedance and supercooled large droplet conditions for comparison as well. This validation, along

with significant research into recommended test methods and advanced component models, has led to a degree of acceptance for use in reducing the cost of development and certification programs.

However, this acceptance does not exist for rotary-wing applications.

LEWICE does not simulate a fully rotational system, but does allow the user to input a number of simple parameters-distance from the hub to the 2D section of interest, rotation speed, and orientation of the plane of rotation (vertical for propellers, horizontal for rotors). LEWICE performs three additional calculations in rotating body cases. The rotation speed is used to calculate an increase in the aerodynamic heating term in the energy balance, the rotational force is included in the ice shedding determination, and the rotational force is used to find the resultant force of the shed ice particle, which is then used to track the particle after it is shed. The rotating body information is not used by the potential flow solver in LEWICE, nor is the rotating body information used by the trajectory equation.

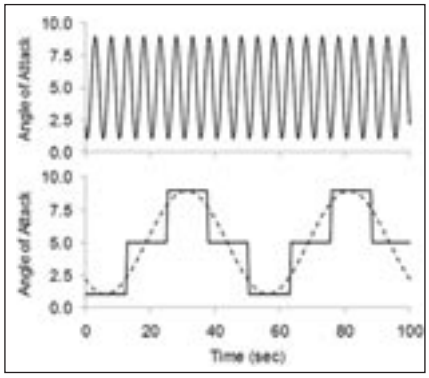

Figure 2. Approach for Simulating Oscillation of Rotor.

LEWICE3D is a suite of codes, developed by NASA and used widely by industry, to determine the amount and location of ice accretion on an aircraft. It is used to calculate water loading on aircraft surfaces so that the size and location of ice protection systems can be determined, to optimize the placement of icing sensors, and to determine ice shapes used in failed ice protection system tests. It is also used to determine corrections for cloud measurement instruments, such as droplet size probes or liquid water content probes on NASA research aircraft.

LEWICE3D uses a Monte Carlo-based collection efficiency calculation using droplet impact counts. Trajectories are calculated using an Adams-type predictor-corrector method. Tangent trajectories and collection efficiencies for simple 2D or 3D regions can also be calculated using a modified version of the 2D LEWICE method. Streamlines are calculated using a 4th-order Runge-Kutta integration scheme.

The ice growth methodology in LEWICE3D uses a single time step strip approach and requires a steady or time-averaged flow solution, supplied by the user. The strip approach is based on the classical Messinger energy balance procedure with an integral boundary layer technique used to generate heat transfer coefficients, and is a modified version of the method used in the 2D LEWICE code applied along streamlines. LEWICE3D supports multi-block structured grids, adaptive Cartesian grids and unstructured grids, as well as panel-based binary-tree grids.

LEWICE3D includes extensions which allow generation of a full 3D ice accretion for surfaces and generation of a new iced surface, calculation of off-body concentration factors, and determination of shadow zones. The program has been parallelized using OpenMP and MPI (message passing interface) to complete jobs faster on parallel machines. The parallel version has been ported to SGI and Linux machines.

However, the current NASA icing codes, LEWICE and LEWICE3D, cannot be applied directly to the ice accretion of rotorcraft flows for several reasons. These codes are acceptable for the majority of fixed-wing applications, such as general aviation, business jets or commercial transports, but there are still shortcomings for some vehicle types, notably rotorcraft.

Past Research in Rotorcraft Icing Codes

The importance of rotorcraft airfoil oscillation during ice accretion was recognized in the early 1980s and NASA sponsored an icing wind tunnel test of a 2D six-inch chord oscillating airfoil. This Sikorsky-run test confirmed that the variation in angle of attack altered the ice shape and produced changes in the drag coefficient. About this same period of time, Sikorsky and the United Technologies Research Center designed, fabricated, and tested in dry air 2D and 3D models with a chord of 17 inches. Meanwhile, as part of an earlier project, Sikorsky designed and fabricated an airfoil test rig to span the NASA Icing Research Tunnel (IRT) test section. This apparatus had a chord of 15 inches and mounted to the upper and lower IRT turntable. Maximum angle of attack for the airfoil was 10 degrees at the maximum operating speed of the IRT of 250 knots (with the model installed and with ice on the model leading edge), with an angle of attack of at least 20 degrees at 150 knots in the IRT.

Model Rotor in the Icing Research Tunnel

To further research on rotorcraft icing, a Government-industry consortium, composed of NASA, Texas A&M University, Bell Helicopter Textron, Boeing Helicopters, McDonnell Douglas Helicopters, and Sikorsky Aircraft, was created to better understand the impact of rotor blades ice accumulation on aircraft performance, increase in vibration and ice shedding. The program was to also validate the industry existing performance models and assessed the benefits of rotor blade scaled model testing.

A two-model approach was selected as the most effective means to accomplish the program goals. A lightly instrumented OH-58 tail rotor that had been modified to operate as a main rotor was chosen as the initial test article.

The initial experimental program was conducted in 1988 in the NASA Lewis Research Center Icing Research Tunnel in which the OH-58 tail rotor assembly was operated in a horizontal plane to simulate the action of a typical main rotor. Ice was accreted on the blades in a variety of rotor and tunnel operating conditions and documentation of the resulting shapes was performed. Rotor torque and vibration were recorded and presented as functions of time for several representative test runs, and the effects of various parametric variations on the blade ice shapes were shown. This OH-58 test was the first of its kind in the United States.

Based on the results of these two tests, it was clear that the CFD methods developed during future studies must include airfoil oscillation and that data must be acquired to validate the method(s). Although investigations into rotor blade ice protection systems continued 1997-99, and commercial use of the IRT continued, NASA essentially put rotorcraft icing research on hold in 1994 to focus on fixed wing following a highly visible fixed-wing accident.

Progress in Tool Development

When opportunity finally arose again at NASA in 2004-2005, the state-of-the-art of subsonic rotary wing icing was quasi-steady and quasi-3D. Grid generation for complex icing shapes was 2D and interactive or crudely automated. There could be a variously loose coupling between the aerodynamics and the ice accretion-but not yet a true, multi-phase solution.

The icing analysis procedure for prediction of performance degradation must address both aerodynamic performance and ice accretion. Aerodynamic performance degradation involves the calculation of the

aerodynamic coefficients of the iced geometry. The section lift, drag and moment characteristics with ice must be accurately known in order to predict the performance degradation from an icing encounter. Lifting line theory is one commonly used method, but momentum source methods coupled with blade element theory are also widely used, as are panel methods. Often, proprietary methods or Navier-Stokes solvers are used to calculate aerodynamics.

NASA's objective was a robust, validated coupling of a rotor performance code with an ice accretion code. The CFD analysis of a clean rotorcraft configuration is well within the range of current technology. Fully time accurate simulations of ice accretion on rotorcraft blades are not currently feasible, however. The complexity of the problem demands high-fidelity tools based on first principles, and a tightly-coupled, physics-based approach is not currently available.

Rotorcraft aeromechanical studies involve coupling the rotor aerodynamics with the structural dynamics of the system. The airloads computed by the CFD solver is used to drive a forced response simulation with the CSD solver. The computed structural deflections are used in the CFD analysis, leading to a change in the airloads. The two solvers are thus inherently coupled. The CFD-CSD coupling may be performed primarily in two ways - loose and tight. In tight coupling, the data is exchanged every time step of the simulation. In loose coupling, the data is exchanged between the two solvers at periodic intervals, typically once per revolution. Since loose coupling is driven by the inherent periodicity in the solution, it is used for analysis of rotors in steady flight conditions.

Coupling Ice Accretion Models with Aeromechanics

One successful approach is an integrated tool set capable of modeling ice accretion and the overall effects of rotor performance. This loosely coupled suite of tools (LEWICE, GT-Hybrid, and DYMORE) has been applied to a representative rotor for detailed study. The entire process (clean rotor grid generation, clean rotor analysis, ice accretion simulations, and iced rotor analysis) is automated and modular. NASA entered into a two-year cooperative agreement with the Georgia Institute of Technology, to develop improved coupling techniques for icing computational fluid dynamics. Georgia Tech was partnered with the Sikorsky Aircraft Corporation.

The project utilizes a 3-D Navier-Stokes analysis and a multi-body dynamics tool, coupled with the GT-Hybrid unstructured Cartesian grid-based flow solver to represent the ice shapes. Several different Navier-Stokes flow solvers have been used in this frame-

work including OVERFLOW, TURNS, and GT-Hybrid. GT-Hybrid, a three-dimensional unsteady viscous compressible flow solver that uses a free wake solver to model the effects of the rotor wake. The flow is modeled from first-principles using the Navier-Stokes methodology. The three-dimensional unsteady Navier-Stokes equations are solved in the transformed body-fitted coordinate system using a time-accurate, finite volume scheme. A third-order spatially accurate Roe scheme is used for computing the inviscid fluxes and second order central differencing scheme for viscous terms. The Navier-Stokes equations are integrated in time by means of an approximate implicit time marching scheme. A Spalart-Allmaras turbulence model is used to compute the eddy viscosity. The flow is assumed to be turbulent everywhere, and hence no transition model is currently used.

A single blade is resolved in the Navier-Stokes domain. The influence of the other blades and of the trailing vorticity in the far field wake is accounted for by modeling them as a collection of piece-wise linear bound and trailing vortex elements. The near wake is captured inherently in the Navier-Stokes analysis. The use of such a hybrid Navier-Stokes/vortex modeling method allows for an accurate and economical modeling of viscous features near the blades, and an accurate "non-diffusive" modeling of the trailing wake in the far field.

Coupled CFD/CSD Analysis for Rotorcraft in Forward Flight

Another icing analysis process that has been developed involves the loose coupling of OVERFLOW-RCAS for rotor performance prediction with LEWICE3D for thermal analysis and ice accretion. This method uses three-dimensional analysis for rotor performance and degradation and two-dimensional analysis for ice accretion. The automated process allows for rapid analysis in a parametric study or for the analysis of an airfoil subject to the many conditions existing on a rotor. For validation, predictions of performance and ice shapes were compared with experimental data for rotors in hover and in forward flight.

NASA entered into a two-year contract with the Boeing Company (Ridley Park, PA), to develop these improved coupling techniques for icing computational fluid dynamics. The project resulted in a process by which OVERFLOW, RCAS and LEWICE can be loosely coupled to assess ice accumulation and rotor performance degradation for helicopters in forward flight, as shown in Figure 1. The system has been tested and evaluated using existing wind tunnel or flight data, and effort is still ongoing. The result is a computational approach for performing high fidelity simulations with ice accretion of rotorcraft blades. The approach is appropriate to address ice accumulation on rotors in flight regimes from hover to high-speed forward flight.

The high fidelity icing analysis approach developed for rotor systems follows three basic steps:

- Establish rotor trim, clean rotor performance and the initial flow field environment using CFD or coupled CFD-CSD as appropriate;
- Extract representative 2D airfoil conditions for blade sections at radial and azimuthal locations and predict ice buildup on the rotor accounting for the diverse operating environment of the rotor;
- Reestablish rotor trim and performance for the iced blades.

Rotor blades experience pitch oscillations as they rotate around the shaft. Pitch oscillations introduce time varying conditions that influence the distribution of ice along the leading edge. The process to predict ice on an oscillating airfoil is built on the premise that the shape is not a strong function of the frequency of the oscillation and is predominantly influenced by the mean and amplitude of the pitch variation. With this assumption, the time history of an oscillating airfoil can be represented by a very slow moving blade. Furthermore, if we assume the shape can be approximated by only considering the mean angle of attack and the extreme excursions from the mean, the blade motion can be represented as the series of quasi-static events, as shown in Figure 2.

Once the ice has been established on the blade, the CFD-CSD analysis process is repeated for the iced rotor. The 3D rotor grid is modified to account for the ice shape on the blade. The input to the CSD analysis is also modified. Accreted ice adds to the blade section mass and

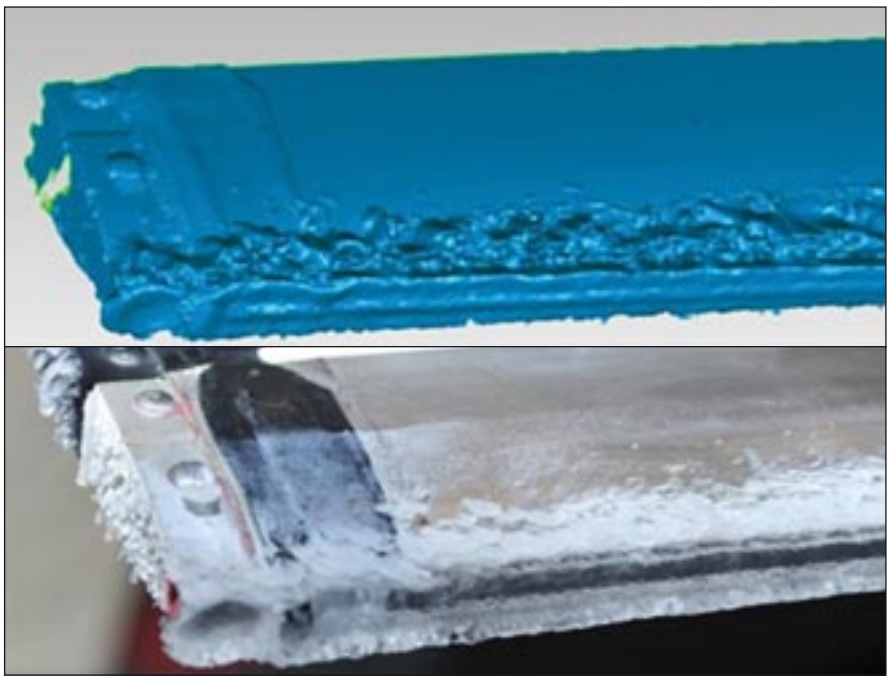

Comparison between scanned data (top) and photograph (bottom) of ice shape on a rotor blade.

chordwise inertia. It is assumed that accreted ice has no effect on stiffness properties. The mass of ice is determined from post-processing the icing analysis, and the placement of the ice is assumed to be at the section leading edge. Updates to the section mass, center of gravity offset, and chordwise inertia are computed and used in RCAS. Rotor performance degradation is obtained by comparing the forward flight performance characteristics of the iced rotor to the baseline rotor.

High Resolution CFD Analysis of Rotorcraft Icing

Additionally, various Eulerian approaches (with both one-way and two-way coupling) for simulating ice accretion have also been examined, but significant work is still required in order to fully demonstrate this alternate method. NASA entered into a two-year cooperative agreement with the Pennsylvania State University to develop improved coupling techniques for icing computational fluid dynamics. Penn State partnered with Bell Helicopter Textron, Inc.

The project applied a zonal approach to the unstructured FUN3D flow solver, extended the existing NASA LEWICE ice accretion formulation to the rotorcraft environment, and coupled this module with the outer CFD flow solution. Initial validation will be conducted by comparison with existing test data. The work will result in an advanced software tool for performing high fidelity CFD simulations with ice accretion of rotorcraft blades. Work is currently ongoing on the thermal modeling for generalized rotorcraft flows, although some issues include the computation of recovery temperature with variable stagnation conditions, transitional flow effects, and working out details to handle them with access to a limited amount of data.

Conclusions

An integrated tool set capable of modeling ice accretion and the overall effects of rotor performance was developed and demonstrated. Key computational parameters were explored, and preliminary results for cases of practical interest were encouraging. Modifications to LEWICE were demonstrated which allow for the retention of previous time-step ice shapes.

Preliminary development of a three-dimensional Eulerian analysis for modeling droplet impingement was also undertaken, to improve more efficient calculation of collection efficiency. The development of a tightly-coupled truly multi-physics approach is still a goal to work towards, but several promising efforts have been undertaken recently. Additional effort is still needed to improve methods for predicting rotor blade shedding and de-icing/anti-icing system performance. An icing analysis process involving the loose coupling of OVERFLOW-RCAS for rotor performance prediction with LEWICE3D for thermal analysis and ice accretion was developed and demonstrated. The method uses 3D analysis for rotor performance and 2D analysis for ice accretion. For validation, predictions of performance and ice shapes were compared with experimental data for rotors in hover and in forward flight.

Studies have also been conducted to examine the effects of grid spacing, grid density, turbulence model, flow-field update frequency and number of spanwise cuts, to name a few. Likewise, simulations of ice accretion prediction and associated rotor performance degradation have been conducted for multiple 2D airfoils and for various 3D rotors in hover and in forward flight. Ice accretion and detailed aerodynamic measurements for 2D clean and oscillating airfoils undergoing both steady and transient behavior was obtained in the IRT. Ice accretion, rotor performance and de-icing/anti-icing system behavior was obtained for a 3D rotating tail rotor in the IRT. For the first time the coupling of an icing code with a computational fluid dynamics code and a rotorcraft structural dynamics code has been demonstrated. The codes and research conducted here are already being transitioned and used by industry.

This article is based on SAE Technical paper 2015-01-2088 by Richard E. Kreeger, NASA John Glenn Research Center; Lakshmi Sankar, Georgia Institute of Technology; Robert Narducci, Boeing Co.; and Robert Kunz, Penn State University, doi:10.4271/2015-01-2088.

CURLED RF MEMS SWITCHES FOR ON-CHIP DESIGN

Microelectromechanical system (MEMS) switches are active components in most electronic equipment. Radio frequency (RF) MEMS are used in wireless personal communication devices, satellite communication, and phased array antennas. MEMS are ideal for these applications because of their low weight, small surface area, low volume, high isolation, large frequency range, linearity, and low power consumption.

While MEMS have many positive attributes, reliability has been a challenge with the charged dielectric; stiction and deformation are two primary causes of failure. In addition, contact welding and contamination of the switch by foreign debris are also problematic. These problems are partly due to the design of the MEMS. In traditional MEMS, the "upper" contact electrode is bridged or flat-cantilevered over the "lower" electrode; there is no significant separation between the electrodes in the off state.

The curled MEMS switch (CMEMS) is a breakthrough technology in on-chip switching design. The switch is a highly flexible and robust curled membrane structure protected by a single-crystal hermetic cover. The curl, corrugation, and cover ensure that the sticking, dielectric charging, and contamination issues associated with traditional MEMS switches are virtually eliminated.

The design of the CMEMS device includes the curled electrode – a corrugated, tri-layered aluminum-silica electrode – and the single-crystal silicon cover. At the heart of CMEMS are the three electrodes. The curled electrode is specially designed with a built-in strain and corrugation to make it roll up and down uniformly. There are two fixed flat electrodes on the substrate. The capacitive (on/off contact) electrode is surrounded on three sides by a pull-down electrode. A voltage, usually a low-frequency square-wave signal, is applied between the curled electrode and the pull-down electrode, creating a force that flattens the curled membrane against the pull-down and capacitive electrodes on the substrate (on state).

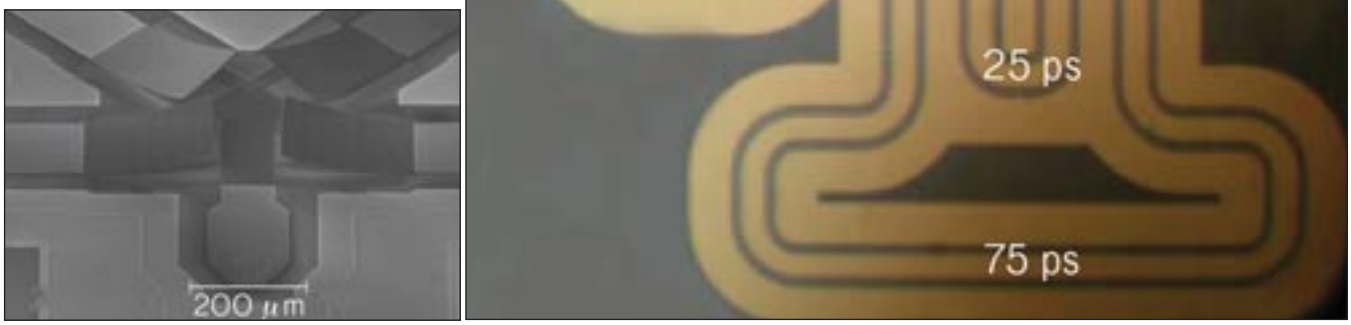

CMEMS can be combined to create a multiswitch "pad." Shown (left) is a four-switch component (without protective caps) that, when combined with three other such components (right), can produce a true time-delay circuit of 16 possible outcomes.

FIVE DAYS ■ THREE CONFERENCES ■ ONE EXHIBITION

EUROPEAN MICROWAVE WEEK 2016
EXCEL LONDON, UK
3 - 7 OCTOBER 2016

EuMW 2016
Microwaves Everywhere

EUROPEAN MICROWAVE WEEK
LONDON, UK
3-7 OCTOBER 2016
www.eumweek.com

EUROPE'S PREMIER MICROWAVE, RF, WIRELESS AND RADAR EVENT

The Conferences (3rd - 7th October 2016)

- European Microwave Integrated Circuits Conference (EuMIC) 3rd – 4th October 2016
- European Microwave Conference (EuMC) 4th – 6th October 2016
- European Radar Conference (EuRAD) 5th – 7th October 2016
- Plus Workshops and Short Courses (From 3rd October 2016)
- In addition, EuMW 2016 will include the 'Defence, Security and Space Forum' 5th October 2016

DISCOUNTED CONFERENCE RATES

Discounted rates are available up to and including 3rd September 2016.

Register NOW and SAVE!

Registration is available after this date and up to 7th October at the standard rate.

The FREE Exhibition (4th - 6th October 2016)

ENTRY TO THE EXHIBITION IS FREE! Register today to gain access to over 300 international exhibitors and take the opportunity of face-to-face interaction with those developing the future of microwave technology. The exhibition also features exhibitor demonstrations, industrial workshops and the annual European Microwave Week Microwave Application Seminars (MicroApps).

EuMA European Microwave Association

Official Publication: Microwave Journal

Organised by: horizon house

Supported by: IET

Co-sponsored by: MTT-S

Co-sponsored by: IEEE

EuMIC 2016
The 11th European Microwave Integrated Circuits Conference
Co-sponsored by:

46TH EUROPEAN MICROWAVE CONFERENCE 2016
The 46th European Microwave Conference
Co-sponsored by:

EuRAD 2016
The 13th European Radar Conference
Co-sponsored by:

Register online now as a delegate or visitor at: www.eumweek.com

Free Info at http://info.hotims.com/61062-780

A significantly lower voltage is applied between the capacitive plates where there are fewer corrugations. The movement of the curled electrode causes a large change in the capacitance between the curled and capacitive electrode. This change in capacitance, from off to on states, provides the switching action for the RF signal.

The robust tri-layer structure, aluminum sandwiched between two silica layers, balances the stress in the curled electrode and provides high conductivity. The unique tri-layer structure prevents elastic deformation, plastic deformation, fracture, and fatigue, all of which are common difficulties with traditional MEMS switches. Corrugations were designed into the switch to induce the proper curl direction (when combined with the intrinsic strain induced by the tri-layering). The corrugated structure has a second function: to reduce the field strength when the electrode is rolled out and in "contact" with the pull-down electrode.

MEMS switches have historically had to deal with contamination. The CMEMS single-crystal silicon cover is strong and is the ultimate gas diffusion barrier protecting the device from contamination. It is designed to protect each switch but at the same time, it enhances the RF properties of the switch. The cover, an intrinsic component of the CMEMS circuit, provides for a very low RF loss and tight confinement of the RF signal.

CMEMS is designed especially for switching alternating-current RF signals above 1 GHz. CMEMS functions over a broad bandwidth, with high linearity and lower loss — a critical parameter for cellphones that rely on battery power — and with the added advantage of small size and weight. One application for which size, weight, and bandwidth are critical is in the RF switching stations found in cellphone ground stations and in satellites. The low loss and immunity from drift are, of course, critical in these applications.

The principal advantage of a switch having a moving metal electrode is the large impedance change that can be achieved. The unique character of CMEMS is the curled electrode that gives by far the largest impedance change of any MEMS or other on-chip switch as it moves from the open curled state to the closed state.

The uniqueness of the CMEMS design:

- Provides a high-power capability for numerous device applications;
- Can carry more information because of its wide bandwidth capability;
- Has a small package dimension, reducing circuit size to much smaller than RF wavelengths, and allowing for true phase shifting;
- Is stable over wide temperature ranges to permit usage in extreme environmental conditions;
- Is extremely reliable — the number of cycles before failure opens up many potential applications;
- Eliminates the sticking problem inherent in other MEMS devices;
- Has a closed loss less than 0.1 dB and open isolation greater than 20 dB over a frequency band of 5 to 40 GHz (for a single packaged switch) — the best-reported results for any MEMS switch over this frequency band.

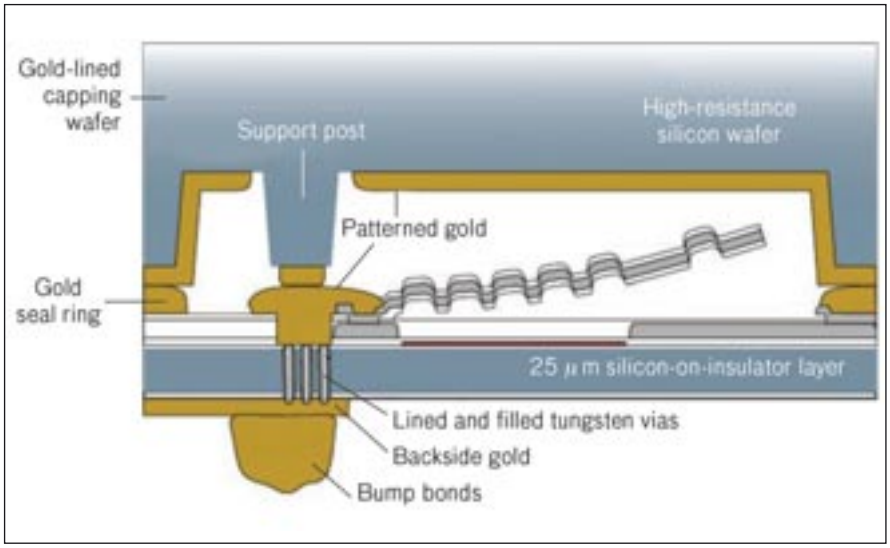

The tri-layer membrane has an internal strain that makes its natural state a highly curled arch, well-separated from the capacitive electrode. This separation results in a very high capacitive difference between on and off states, thus eliminating any potential for stiction or leakage in the off state. The single-crystal cover is an integral part of the RF electronics, and provides all connections to the switch in the same footprint size, eliminating bulky contacts. The gold ring is thermocompressed to form the hermetic seal. The interior chamber is RF isolated, making it an ideal RF waveguide.

RF MEMS switches are ideally suited for use in wireless personal communication devices, satellite communication, and phased array antennas. The CMEMS design not only dramatically reduces the failure modes typical of other MEMS devices, but significantly improves the capabilities as well. The prime example of an application for CMEMS is a true time-delay circuit for a phased array antenna. For the first time, a MEMS switch is compact, low loss, and reliable enough to eliminate the need for the current multiplicity of amplifiers. By using a low-loss phase shifter at each pixel, a single power source can be split among all pixels. Low-cost arrays could make possible their use on vehicles and as fixed sensors.

This article was contributed by the Advanced Imager Technology Group at the Massachusetts Institute of Technology Lincoln Laboratory in Lexington, MA. For more information, contact Dr. Carl Bozler at bozler@ll.mit.edu; 781-981-4637.

Design Software Supports BAE System's Mixed-Signal Chip Design

BAE Systems is a global defense and aerospace company, delivering products and services for air, land, and naval forces, as well as electronics, information technology solutions, and customer support services. In partnership with AWR Corp. (El Segundo, CA), MIT, Cornell University, and Alcatel-Lucent Bell Labs, BAE Systems has been working to produce a new breed of devices that embeds photonic devices into silicon-based integrated circuits (ICs), enabling computer chips to perform digital, radio frequency, and photonic functions in a single chip.

Analog Office provides high capacity and fast layout for mixed-signal design.

The Electronic and Photonic Integrated Circuits (EPIC) program is funded by the Defense Advanced Research Projects Agency (DARPA) to produce a mixed-signal electronic/photonic application. The research is being built on by Alcatel-Lucent Bell Labs, which demonstrated the first CMOS silicon-based tunable optical waveguide equalizer, a major step toward high-density, low-cost silicon chip-based optical networking devices.

BAE Systems is taking a mature electronics process in complementary metal oxide semiconductor (CMOS) and adapting it to add complex photonics functions ranging from the photonic processing of massive amounts of RF bandwidth, to extremely high-speed digital interconnects. The company has developed a range of monolithically integrated CMOS-compatible photonic devices including ultra-low-power-consumption silicon ring optical modulators, fourth-order narrowband optical filters with tunable passbands and center wavelengths, and silicon-germanium (SiGe) waveguide photodetectors. The design of these mixed-signal chips is extremely complex, and accurate behavioral models are key to developing and producing high-quality performance at a reasonable cost.

BAE Systems uses the Analog Office® RF integrated circuit design suite from AWR Corp. to develop RF and microwave photonic applications, and AWR provides consulting services for the development of models and process design kits (PDKs). AWR has been working closely with photonics designers at BAE Systems and Bell Labs to develop accurate behavioral models based on the EPIC data. The two teams are also working together to create a PDK that will enable accelerated silicon tape-out of the photonics chips. In addition, AWR's Analog Office software is being used to extract the models.

The integrity of the electrical and physical model data is often an issue between foundry customers, foundries, and EDA vendors. The PDKs are customized for the AWR open design platform with its unified data model, and carefully developed from supplied technology files, device models, and design rules specifically for Analog Office.

The Analog Office design suite is specifically architected and optimized from the ground up for next-generation radio-frequency integrated circuit (RFIC) designs. Designers of RFICs and analog ICs use the software to control and integrate tools to capture, synthesize, simulate, optimize, lay out, extract, and verify RFIC and analog designs from the system level through to final tape-out. The integrated environment features concurrent interconnect-driven and RF-aware design methodology for interactivity and accuracy. The solution is built on AWR's open high-frequency design platform. AWR PDKs are subjected to an extensive level of validation at both cell and circuit level to ensure quality and conformance to best-in-class design methodologies for high-frequency RFIC designs.

For more information, visit ***http://info.hotims.com/61062-542****.*

Precision Assembly of Systems on Surfaces (PASS)

Functionalized carbon nanotube devices could be used as chemical sensors.

U.S. Army Research Office, Research Triangle Park, North Carolina

Chemiresistors represent a powerful class of chemical sensors that can be readily integrated into any electrical system, can be miniaturized, are readily multiplexed, and take nearly zero-power to operate. One of the greatest limitations to these sensors is a lack of selectivity, which is the electronic equivalent of noise. Interference from large varying background signals, such as humidity, can compromise the sensor signal to a point where there is no useful data. To address this challenge, new ways to integrate molecular constructs into carbon nanotube compositions that produce enhanced selectivity to certain molecules or classes of molecules were investigated to increase the signal to noise level in chemical sensors.

To realize the full diversity of the first row transition metal sensors, metal porphyrin complexes were targeted. These materials have extended π-electron systems that make them ideal candidates to bind through non-covalent mechanisms to the surfaces of carbon nanotubes. To promote strong interactions, a porphyrin system containing fused pyrene systems was chosen. Although the synthetic procedures were reproducible and it was possible to make the regioisomeric Co^{+2} complexes of these molecules, it was found that the tendency to self-associate precluded their ability to form strong complexes with carbon nanotubes. As a result, it was found that functionalization of single walled carbon nanotubes (SWCNTs) with these molecules has minimal effects on their response to specific chemicals of interest.

To properly evaluate the ability to utilize porphyrins to create selectively modified surfaces for chemical sensing, a study was conducted wherein the first row transition metal series of complexes (Figure 1) based on tetraphenylporphyrin (tpp) were prepared and used to functionalize the SWCNTs. Previous studies on porphyrins in chemical sensing note that despite their promise for this application, a drawback that limits their usage is that they are relatively unselective. However, earlier studies with sensors fabricated from porphyrin-CNT composites measured chemiresistive responses of only 2-3 metal centers to only 4-5 different analytes. A more comprehensive study on

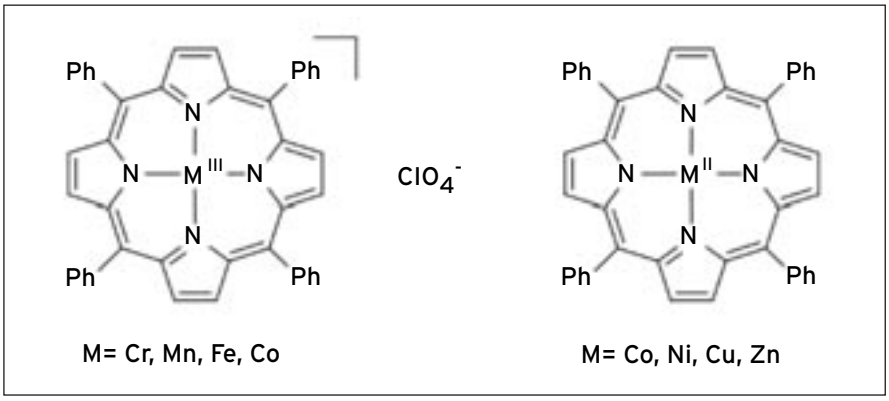

Figure 1. Chemical structures of metalloporphyrin complexes employed in the chemiresistive sensor array. Axial H_2O ligands have been omitted for clarity

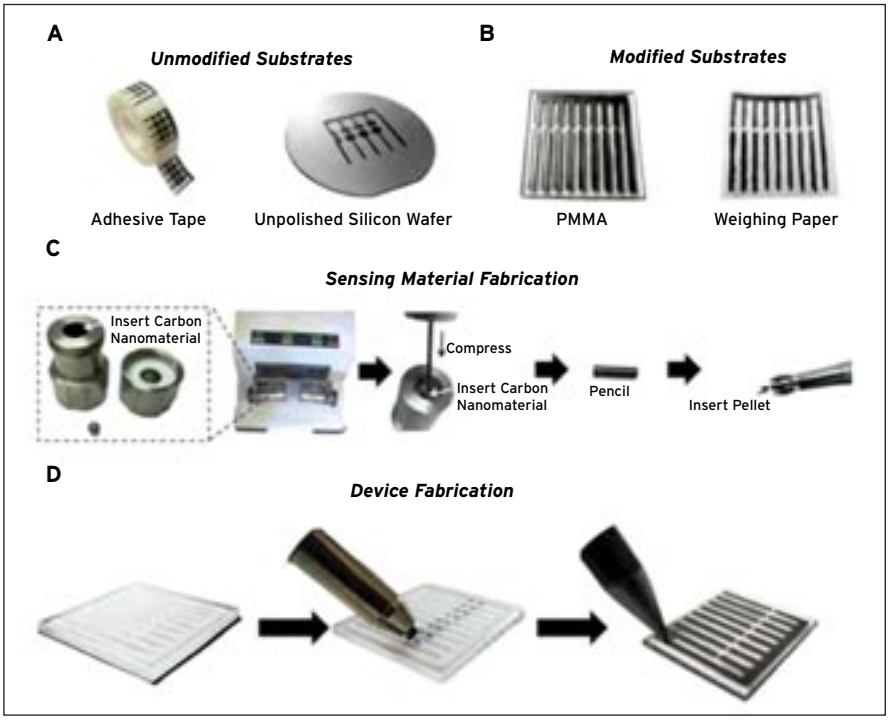

Figure 2. Fabrication of chemiresistive chemical sensors by drawing. Sensing materials (SWCNT-based) and graphite as electrodes were both deposited by mechanical abrasion to yield fully-drawn, chemiresistive gas-sensors on various A) unmodified substrates such as adhesive tape and unpolished silicon wafer, and B) laser-etched substrates such as PMMA and weighing paper. C) Fabrication of the sensing material consists of mechanically mixing and compressing SWCNT composites into a pellet. D) Three-step fabrication of fully drawn chemiresistive sensors on PMMA: laser-etch PMMA, deposit SWCNTs by abrasion (sensing material), and deposit graphite by abrasion (electrodes).

the chemiresistive responses has been completed and it was found that the responses of metalloporphyrin-SWCNT-based sensors to vapors of various volatile organic compounds (VOCs) were strong and were subjected to statistical analyses that enabled the successful classification of representative VOCs into five different categories (aliphatic hydrocarbons, alcohols, ketones, aromatic hydrocarbons, and amines) with 98% accuracy.

With the exception of amines, which are capable of strong charge transfer interactions, the basis of classification appears to correlate with the differences in the solubility properties of the porphyrin compounds in the various VOCs as solvents. This feature suggests that solvent vapors modulate the strength of interactions between the porphyrins and the nanotubes. These results further demonstrate the potential for porphyrin-functionalized SWCNT-based electronic noses for applications in inexpensive, portable chemical sensors for the identification of VOCs.

The ability to create on demand chemical sensors with minimal infrastructure offers a useful capability in support of covert and/or battlefield applications. The object, therefore, is to develop a rapid, scalable, portable, and cost-effective approach for the fabrication of fully-drawn chemical sensing arrays on a variety of different substrates (e.g., paper, plastic, and undoped float zones silicon wafer). This approach is entirely solvent-free, requires only small amounts of sensory materials, and is capable of producing highly-sensitive chemical sensors.

This approach has been demonstrated in the context of sensing and differentiating a variety of vapors at ppm concentrations. The demonstration employs solid composites of single-walled carbon nanotubes (SWCNTs) and small molecules as the sensing material and graphite as electrodes utilizing a previously established method to generate sensing materials, or PENCILs (Process Enhanced NanoCarbon for Integrated Logic), by the mechanical mixing of SWCNTs with commercially available small molecules (solid or liquid). A technique called DRAFT (Deposition of Resistors with Abrasion Fabrication Technique) was then used to deposit these materials on a variety of substrates. Sequential deposition by mechanical abrasion of sensing materials and commercial graphite pencils on various etched and non-etched substrates yields precisely fabricated fully-drawn chemiresistive sensing arrays (Figure 2).

The performance of the arrays were benchmarked against those created using conventional metal based electrodes. It was found in all cases that the fully drawn sensors were able to match the performance of those on similar substrates with metal (Au) electrodes.

This work was done by Timothy M. Swager of Massachusetts Institute of Technology for the Army Research Office. ***For more information, download the Technical Support Package (free white paper) at www.aerodefensetech.com/tsp under the Manufacturing/Automation category.*** *ARL-0193*

Development of a Novel Electrospinning System with Automated Positioning and Control Software

System automates the production of fiber scaffolds through a single user interface.

Naval Medical Research Unit, San Antonio, Texas

Electrospinning is a nanofiber fabrication technique that has grown in popularity due to its potential in numerous biomedical applications. The process uses an electrical charge to draw ultrafine fibers from liquid polymer solution to form a non-woven fiber scaffold. The polymer fiber diameters can range from millimeters to as small as nanometers in scale.

The primary elements of an electrospinning system include: a dispensing needle (or spinneret), a high-voltage power supply (5 to 50 kV), a syringe pump, and a grounded collector. The polymer solution in the syringe is extruded from the spinneret at a constant rate. As high voltage is applied at the spinneret, a cone is formed at the tip. This phenomena, known as the "Taylor cone", is caused by the balance between electrostatic forces and the surface tension of the polymer. With sufficient voltage, electrostatic forces will overcome the surface tension, ejecting a thin jet of polymer from the spinneret (Figure 1). As the polymer stream travels to the collector, the solvent dries and the stream experiences whipping instabilities, which promotes the elongation and thinning of the fiber before deposition on the collecting surface.

The electrospinning hardware consists of three sub-systems: the gantry components, the syringe pump, and the high voltage power supply. Control of the three sub-systems is achieved using a personal computer (PC) running custom software developed in LabVIEW™.

Three axes of translational movement were required to adjust the position of the dispensing needle relative to the collecting surface. Each axis consists of a stepper motor that rotates a lead screw to move a plate along the track of a linear actuator. The x-axis and y-axis are coupled and move the collector plate, while an independent z-axis moves the dispensing needle.

The linear actuators have a lead screw, with a pitch of 10 turns per inch, rigidly attached to a mounting plate. The assembly lies inside a track enclosed on three sides. Each slide has adjustable limit switches on either end of travel to provide a soft emergency stop prior to the slide reaching a hard physical limit. The x- axis and z-axis slides have a travel distance of 15" and the y-axis slide has a travel distance of 20".

The stepper motors used in the electrospinning system each have an integrated driver and controller. The motors have a 1.8° full step resolution and are capable of generating microsteps as small as 1/256 of a full step. The encoder generates 1250 counts per revolution and allows the position of the gantry to be controlled and measured with a resolution of ~ 2 microns. The motor assembly is also programmable with 4kB of memory, and prewired to receive inputs from the limit switches at either end of the travel distance.

An RS232 kit provides a communication link between the motors and the PC. The RS232 kit converts serial communication from the PC to an indexed RS485 protocol, which allows a single PC serial port to communicate with multiple stepper motors independently. A 36V power supply is used exclusively for

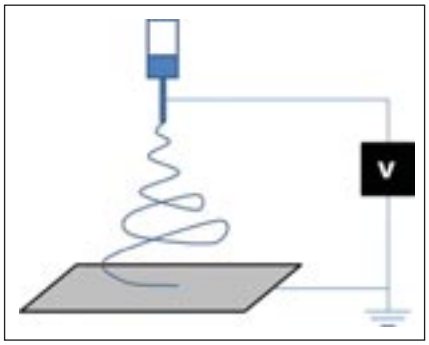

Figure 1. Electrospinning schematic. A high voltage is applied to a polymer solution dispensed from a syringe pump. Electrostatic forces stretch the droplet at the needle tip, and a thin jet of polymer is ejected from the cone, which dries and whips as it travels toward the grounded collector plate.

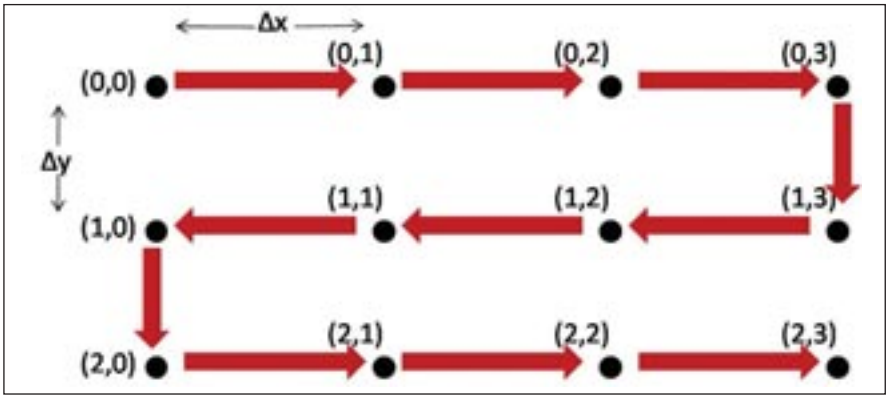

Figure 2. Sample trajectory for patterned spinning. The operator specifies the gap distances (Δx, Δy), speed, pause time (if desired), and coordinates for locations that require a pause or a change in direction.

the gantry motors. The power supply input is 120VAC, and it outputs 36V at 8.5A (300W).

Polymer solution is delivered to the energized needle with a high-precision syringe pump with dual syringes. The instrument can be programmed to operate as a single dispenser (one solution and one syringe), dual dispenser (two solutions in two separate syringes), or continuous dispenser (two linked syringes and one solution). The syringe pump uses positive displacement providing better than 99% volumetric accuracy. The step resolution is 48,000 steps per stroke of the pump, independent of syringe size.

The high voltage power supply provides the necessary voltage differential between the needle tip and the collector plate to eject the polymer fiber from the Taylor cone. The voltage required to spin fibers varies widely depending on the particular polymer and solvent combination; typical values from the literature range between 5 – 50 kV.

Communication with the high voltage power supply was established with a data acquisition unit (DAQ), which receives commands from the LabVIEW™ interface and sends a scaled control signal to the high voltage supply. The high voltage output is connected to the needle using a charged adapter disc held in place with a setscrew, and the power supply ground is connected to the collector. A second wire with an alligator clip connects the dispensing needle to ground whenever the power supply is off, to ensure the system is fully discharged when not in use.

At any point after initialization, the gantry can be moved in x, y or z directions. From the interface, the operator enters a distance value in the dialog box and presses the control indicating the desired direction of movement. Once the gantry is initialized, the operator also has the option to load a spreadsheet with patterning parameters to instruct the gantry to move along a specified path. In a simple example of its application, the gantry can traverse a rectangular space by moving along one dimension, alternating direction with each row and pausing at intervals (Figure 2). The operator enters x and y distances values, which define the arbitrary coordinate grid containing the node locations of a pause or change in direction. Other input parameters include speed and time to run, which is linked to the syringe pump. Once the gantry has reached the last node specified in the routine, the program executes the path in reverse. The collector plate will run this forward and reverse sequence continuously until stopped by the operator or at the end of a pre-defined period of time.

This work was done by Bridget Endler, MS; Roy Dory, MS; Tony Yuan, MS; and Mauris DeSilva, PhD for the Naval Medical Research Unit. ***For more information, download the Technical Support Package (free white paper) at www.aerodefensetech.com/tsp under the Manufacturing/Automation category.*** *NRL-0066*

Advanced Multifunctional Materials for High Speed Combatant Hulls

A new additive manufacturing process for producing composite materials with prescribed RF properties.

Office of Naval Research, Arlington, Virginia

Currently small boat combatant design focuses primarily on speed and maneuverability. It would be advantageous to expand these capabilities to include reduced radar cross-section, and enhanced survivability to blast and ballistic threats for both the structure and warfighters.

Investigators from the University of Delaware along with Navy partners at the Naval Surface Warfare Center developed the material building blocks necessary to realize hull materials for small boat combatants that combine structural properties with integrated radar absorption and enhanced ballistic protection. Specifically, additive manufacturing methodologies were used to develop new multifunctional materials that can be manufactured in a flexible, scalable and cost effective manner. These new materials and processing

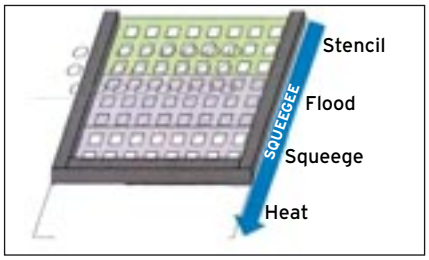

Figure 1. Screen printing process

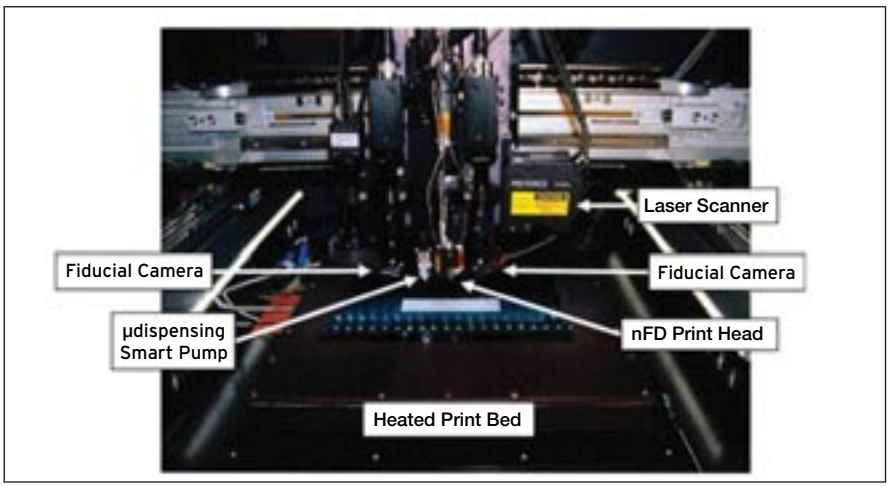

Figure 2. Micro dispensing system

methods will be part of a library of core material building blocks that can be optimally combined in a stackable layup to produce the next generation of multifunctional hulls.

Most high speed combatant hulls are traditional sandwiched core designs constructed from a foam or balsa wood core sandwiched between two composite face sheets. Current methods to augment these structures with ballistic capabilities employ arrays of small panels, made typically from metal, carbon, glass or high strength polymer fibers, bolted onto the outer surface. One clear disadvantage of this approach is the large {>100%) increase in both size and weight. The use of outer panels constructed from high strength polymer fibers, such as Dyneema or Spectra, has shown the most promise in adding ballistic performance while minimizing additional weight. Similarly, most radar absorbing hulls are constructed by adding layers of radar absorbing materials (RAM) treatments to the outer surfaces of a traditional hull design. There are currently no examples of hull materials that combine structural, ballistic and radar absorbing functionalities.

The technical approach to solving that problem was to employ scalable screen printing to print patterns of functionalized custom inks and pastes to composite materials. The proposed effort was modeling and simulation driven guiding the selection of appropriate composite materials, inks, additives and printable patterns to create design methodologies that can be followed to produce composite materials with well-defined electromagnetic, structural and ballistic properties.

To realize a multifunctional hull material that minimizes weight, a number of advanced composite materials were used in addition to standard woven glass and carbon based composites. These included woven glass fabrics and Kapton, a polyimide film that's a common dielectric substrate used for printing electronics, as well as high strain rate polymer composites such as Dyneema HB26 or Spectra Shield.

Three types of electromagnetically functional inks were also explored: resistive inks, high dielectric constant inks, and magnetic inks.

To tailor structural, ballistic and electromagnetic properties within a composite required exploring new manufacturing methods, namely screen printing and micro-dispensing. Screen printing is an additive manufacturing method that utilizes a mesh screen, a flood, and a squeegee, as seen in Figure 1. The mesh screen that was used contains a desired geometrical pattern that was deposited onto the substrate. When the flood is actuated, it deposits ink across the surface of the screen, the screen is then lowered to a snap-off height above the substrate, and the squeegee actuates to deposit the desired pattern. The substrate is then heated to cure the deposited ink. This process allows for a designed pattern to be repeatedly deposited onto multiple substrates in a short period of time.

Micro dispensing is a process of additive manufacturing that utilizes a dispensing head to precisely deposit a material. The micro dispensing system that was used in this research was an nScrypt 3Dn-300, pictured in Figure 2. The system is capable of utilizing two different types of dispensing heads for depositing a wide variety of materials. The implementation of two printing heads allows for the printing system to toggle between printing two materials at once. These materials may also be swapped out mid-print in order to incorporate varying properties within one structure.

The results of this research are broken down into three categories based on the nature of the ink used. Specifically, detailed results are provided for high dielectric constant loaded composites, magnetically loaded composites, and resistively loaded composites.

This work was done by Mark S. Mirotznik of University of Delaware for the Office of Naval Research. ***For more information, download the Technical Support Package (free white paper) at www.aerodefensetech.com/tsp under the Manufacturing/Automation category.*** *ONR-0034*

Multifunctional Shear Pressed CNT Sheets for Strain Sensing and Composite Joint Toughening

Investigating the critical fabrication aspects and potential applications of a novel carbon nanotube material named shear-pressed sheet.

Air Force Research Laboratory, Arlington, Virginia

The main goal of this work is to obtain a scientific understanding of the possibilities provided by, and the behavioral features of, a novel type high performance carbon nanotube (CNT) reinforced composite material incorporated in the interfaces of composite laminates and bonded joins with the following two purposes: (a) providing enhancement of the interlaminar fracture toughness and strength and (b) serving as a continuous strain monitoring sensor.

The material under investigation is a relatively thin (in the range of several hundred microns), high CNT volume fraction, shear-pressed sheet (SPS) fabricated from the vertically grown aligned CNT array (a.k.a. "CNT forest"). The intrinsic high fracture toughness of composites reinforced with such CNT SPS should provide significant increase in the interlaminar fracture toughness of composite laminates and bonded joints. Simultaneously, the piezoresistive nature of the aligned CNTs and their interconnected networks opens new opportunities for monitoring both the strain and progressive failure in the composite joints. The stated principal outcome of this research was to establish a starting point for the future development of field deployable multifunctional CNT SPS interface-enhancing materials enabling, at the same time, for strain sensing of composite laminates and bonded joints of aerospace structures.

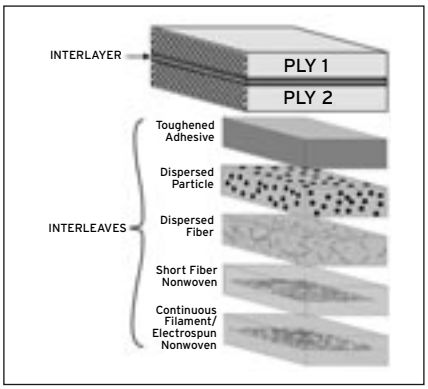

Illustration of the interlayer concept and classification of the known interleaves comprised within interlayer.

The interleaf material is fabricated from CVD vertically grown CNT arrays by the shear pressing method. The shear pressing is realized here on a specialty automated device which allows one to delicately control the CNT array alignment, CNT volume fraction and the shear pressed sheet (SPS) thickness. The produced thin dry SPS can be strategically placed within some region between composite plies and, after conventional laminate fabrication it becomes its integral part. Under this scenario, the SPS can be partly or fully impregnated during the cure process with the resin which is already contained in the prepreg plies. An alternative manufacturing approach could be to first impregnate the SPS preform with some other, desirably lower viscosity, resin and partially cure it, then embed the "SPS prepreg" between the plies of composite and complete the manufacturing cycle.

Extensive experimental results show how the Double Cantilever Beam (DCB) testing methodology can be used to evaluate the effect of different CNT SPS interleaves on Mode I interlaminar fracture toughness of conventional carbon/epoxy laminated composites. The experimental studies also included traditional optical microscopy and SEM imaging of the fractured DCB samples. They showed that the delamination propagation path is dramatically altered in the presence of CNT SPS interleaves. It changes from a nearly straight one to highly tortuous; the latter one typically consists of a sequence of jagged or saw-tooth type microcracks often combined with even more subtle sub-micro scale cracks developing within the interleaf, and with microcracks propagating between the interleaf and adjacent composite ply. The overall delamination fracture mechanism shows highly variable from sample to sample and very sensitive to such factors as CNT functionalization, epoxy resin viscosity, cure cycle, the resin infusion technique into the SPS, to the presence of residual voids, and other fine manufacturing peculiarities.

Overall, results of this research in the part of enhancing fracture toughness of traditional laminates by embedding CNT SPS interleaves are very encouraging. They showed that both dry and pre-infused CNT SPS interleaves significantly, up to two times, increase the critical strain energy release rate of the baseline non-interleaved laminate. The non-functionalized, plasma treated and acid treated SPSs were used. Both functionalization methods maintained the high alignment and aspect ratio of the CNTs.

Although adding the CNT functionalization step does not result in further significant toughening versus the non-functionalized interleave case, the characteristics of the fracture surfaces appear to be dramatically different. As evidenced by the much "smoother" load vs. displacement curves, the pre-infused SPS interleaves show better ability than the non-interleaved and dry SPS interleaved laminates to resist catastrophic failure. Apart from the Mode I fracture toughness performance (which was in the focus of this study), the CNT SPS reinforcements provide high dimensional stability to the interleaves and structural joining elements. This feature may be especially beneficial for interfaces and joints in high-precision devices and structures (particularly, miniature ones) which require very thin preforms with well-defined dimensions - a requirement that may be difficult to satisfy with traditional adhesives and bonding methods.

This work was done by Dr. Alexander Bogdanovich and Dr. Philip Bradford of NC State University College of Textiles for the Air Force Research Laboratory. ***For more information, download the Technical Support Package (free white paper) at www.aerodefensetech.com/tsp under the Manufacturing/Automation category.*** *AFRL-0242*

Cov ToC

LAST CHANCE! Entry deadline: July 1, 2016

Connect on social media: #CTF2016

"THE BEST WAY TO PREDICT THE FUTURE ...IS TO CREATE IT."

—ABRAHAM LINCOLN

Altering the Future

2015 AEROSPACE & DEFENSE CATEGORY WINNER

N5 FILO HAZARDOUS GAS DETECTOR

The microsensor arrays on a single chip could replace multiple conventional macro scale gas sensors used in portable multi-gas detectors. These new sensors are small, accurate, low-power, and capable of detecting multiple gases at the same time. This product will enable industrial workers, first responders, and soldiers to quickly detect multiple types of dangerous gases using a mobile device.

"Winning the Create the Future Design Contest award was a big recognition for the N5 team. We have received follow-up inquiries and leads after receiving the award," said Abhishek Motayed, president and founder of N5 Sensors.

WILL YOUR DESIGN BE NEXT?

Start Creating the Future at:

www.createthefuturecontest.com

Create THE Future

DESIGN CONTEST 2016

PRINCIPAL SPONSORS

COMSOL

MOUSER ELECTRONICS

ANALOG DEVICES

intel

CATEGORY SPONSORS

Maplesoft

imagineering inc.

QOSINA

DYMAX

PRIZE SPONSORS

hp

NVIDIA

SUPPORTING SPONSOR

FLC Federal Laboratory Consortium for Technology Transfer

Upmast Radar Systems

Kelvin Hughes
Enfield, UK
+44 19 9280 5200
www.kelvinhughes.com

Kelvin Hughes recently installed its new SharpEye™ upmast radar system on four new vessels commissioned by the Trinidad and Tobago Defence Force. The Damen Stan Patrol 5009 Coastal Patrol Vessels are all now fitted with a Kelvin Hughes Advanced Surveillance System incorporating a SharpEye™ X-Band radar, located upmast in a carbon composite housing with a stealth profile, as well as a tactical radar display. The four craft - the TTS Speyside, Quinam, Moruga and Carli Bay - will patrol Trinidad and Tobago's coastal waters and are also capable of operating in its Exclusive Economic Zone.

The SharpEye™ radar was selected as the surveillance radar due to its superior target detection capability, especially in poor weather conditions such as heavy rain and high sea states. Dedicated primarily to surface search and surveillance to counteract illegal activity, the radar will also be used in support of the vessels' navigational magnetron radar to provide the safety and situational awareness required in high clutter conditions.

With its longer range target detection capability and low power output - reducing the probability of detection by ESM equipment - the SharpEye™ radar will enable the craft to remain out of visual sight and out of conventional radar detection range whilst still being able to track and monitor vessels under investigation.

The original order for the SharpEye™ radar systems was placed by Alphatron Marine BV of The Netherlands who was assigned as the integration partner for Damen Shipyards. With deliveries and sea trials conducted between April and October of last year, the program was concluded in November and both the radar and the patrol craft are now in service.

The Damen Stan Patrol 5009 is the first "Sea Axe" patrolboat, which means that the hull is designed according to the "Axe Bow Concept". The keel line slopes down forward and the sheer line slopes up – strongly resembling the blade of an axe. Due to the oversized hull of the Damen Stan Patrol 5009, it was possible to place the wheelhouse at the position where the ship motions are least – approximately one third from the stern. This creates the best possible working environment for the crew. The engines are flexibly mounted, to obtain low vibration levels.

The Damen Stan Patrol 5009 can be equipped with Caterpillar or MTU engines.

For flexibility, efficiency and redundancy, four fixed pitch propellers, two hydraulic bow thruster and two rudders are installed. Depending on the choice of engines, the maximum speed of the Damen Stan Patrol 5009 varies between 22.5 and 32 knots. The range at patrol speed (10-16 knots) is approximately 3,000 nautical miles.

For Free Info Visit
http://info.hotims.com/61062-509

Virtual Environment-Based Training Tools

Charles River Analytics
Cambridge, MA
617-491-3474
www.cra.com

Charles River Analytics Inc., a developer of intelligent systems solutions, has received a follow-on contract from the US Navy to develop more efficient training tools in virtual environments. Shiphandling Educator Assistant for Managing Assessments in Training Environments, or SEAMATE, supports experienced instructors as they monitor and interact with larger numbers of students in the classroom, increasing training efficiency while reducing costs and maintaining effectiveness. The contract is valued at just under $1 million with a contract extension option close to $500,000, if exercised.

While they significantly reduce the need for costly live training at sea, virtual shiphandling trainers such as the Navy's Conning Officer Virtual Environment (COVE) depend heavily upon expert mariners, with individual instructors typically working with only a single active student at a

time. With the limited number of available expert mariners, this one-on-one training requirement makes it difficult to realize the full benefit of virtual training systems. Emerging automation technologies, such as Intelligent Tutoring Systems (ITS), will offload many manual instructor tasks, but introduce new supervisory challenges for instructors monitoring multiple students simultaneously. Charles River is developing SEAMATE to more efficiently meet these new training demands, enhancing the overall efficacy and scalability of COVE training.

"In SEAMATE, we're developing supervisory displays that help shiphandling instructors work with more students at once," explained Dr. Ryan Kilgore, Vice President of Charles River's Human Effectiveness division. "The Navy's knowledgeable instructors are invaluable to the training process, and we're developing tools that extend their training expertise to a larger number of students. We're evaluating how instructors dynamically shift their attention and engagement across students and decide when and how to provide specific coaching and feedback. SEAMATE will let instructors monitor more students in parallel, and help them quickly pivot to one-on-one coaching as though they've been watching over a single student's shoulder for the whole training exercise."

SEAMATE includes a mobile technology dashboard through which a trainer can monitor multiple students' performance at once. It notifies a trainer when a student may need assistance, improving awareness of individual progress.

Beyond the SEAMATE effort, Charles River is developing a number of tools to help improve training. MAGPIE helps provide a more powerful and personalized training experience through an adaptive, game-based environment. TMT provides training on tourniquet technology to aid warfighters treating injuries on the battlefield.

For Free Info Visit http://info.hotims.com/61062-507

Cov ToC

New Products

Handheld Marking Unit

The new FlyMarker® mini is the fourth generation of the battery-operated, FlyMarker® dot peen marking system from Equipment Sales Co. (Sioux City, IA). Housed in an ergonomically designed, compact unit weighing just 6 lbs, the mini can be carried around with no power or air cables needed. Its strong magnet and powerful battery produce durable and unforgeable markings on nearly any material ranging from plastics to aluminum to steel. The versatile mini also marks round parts, with automatic height compensation up to 5mm.

The marking files can be programmed via self-explanatory software on the unit itself and includes storage space for several hundred files. Alternatively, one can create the marking files using optional PC-software and then transfer to the mini using its built-in USB-interface. Logos, data matrix codes, integrated bar code scanners, and solid column frames for conversion to a tabletop unit are just a few of the optional accessories.

For Free Info Visit http://info.hotims.com/61062-511

Radiation Tolerant MIL-STD-1553 Solutions

Data Device Corporation (DDC) (Bohemia, NY) has introduced two new +3.3V completely integrated radiation tolerant MIL-STD-1553 terminals that include transceivers, transformers, protocol and memory. Total-Space ACE offers full BC, RT, MT, and RT/MT functionality to interface directly to a host processor, while the Total-Space RT is an RT only terminal ideal for interfacing with systems without a host processor, such as FPGA and simple logic. Both versions feature an extended -55°C to +125°C temperature range, and 300 Krads TID (Total Ionizing Dose) and >85 MeV SEE (Single Event Effects) radiation hardening, required for the extreme environmental conditions encountered in mission critical space applications.

For Free Info Visit http://info.hotims.com/61062-529

XMC Module

Innovative Integration (Camarillo, CA) introduced the XU-TX, an XMC module featuring two, AC-coupled, single-ended 16-bit DAC outputs with programmable DC bias. The DAC devices employ support synchronization and interpolation and their unique output circuits allow improved frequency synthesis in the 2nd and 3rd Nyquist zones, to shift of the Nyquist null frequency in the output spectrum by a factor of two. The DAC ICs may be clocked at up to 5.1 GHz via an onboard, ultra-low-jitter PLL.

A Xilinx Kintex UltraScale XCVU060/085 FPGA supported by 8 GB DDR4 and 4 MB of QDRAM memory provides a high performance DSP core for demanding applications such as radar and wireless IF generation. The close integration of the analog IO, memory and host interface with the FPGA enables realtime signal processing at rates exceeding 7000 GMAC/s.

For Free Info Visit http://info.hotims.com/61062-519

6U VME Single Board Computer

Acromag's (Wixom, MI) XVME-6510 is a high-performance 6U VME single board computer based on the 4th Generation Intel® Core™ i7 processor and utilizes the Intel 8-Series QM87 PCH chipset for extensive I/O support. Two ruggedized SODIMMs offer up to 16GB of high-speed DDR3L removable memory plus 32GB of flash memory.

The air-cooled XVME-6510 features dual PMC/XMC sites, DVI-D display, and programmable CPU power limits for heat sensitive applications. Extended temperature models are available for operating in a -40°C to +75°C range. The two PMC/XMC sites can be used in any combination. An optional P0 connector allows two Gigabit Ethernet connections. Forego one PMC/XMC module and add the optional XBRD-9060 I/O expander module and increase I/O on the front panel and add two SSD mSATA drives. A XVME-9640 rear-transition module for easy access to all P2 connectors' I/O signals is also optional.

For Free Info Visit http://info.hotims.com/61062-518

3 KW DC Power Source

Intepro Systems (Tustin, CA) recently introduced the PSI 9000 2U programmable DC power source, providing a 1-3 KW supply with a feature set typically found in higher power 3U systems. The PSI 9000 2U power source features an interactive system with touch panel menu navigation that simplifies set up and storing to test profiles. The high-efficiency (up to 93%) unit includes an integrated true function generator. For user convenience, complex test sequences can be loaded from the system and saved to a standard USB flash drive.

A unique feature of the PSI 9000 2U power source is its auto-ranging output that is capable of delivering a three-times higher output current at reduced voltages. Additional features of the RoHS-compliant PSI 9000 2U power source includes a galvanically isolated analog interface for voltage, current and power programming and monitoring; digital plug-and-play modules supporting RS232, Ethernet, CANopen, Modbus TCP, Profibus, Devicenet; and IEEE/GPIB and SCPI command language support.

For Free Info Visit http://info.hotims.com/61062-512

Product Spotlight

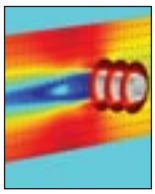

COMSOL MULTIPHYSICS FOR SIMULATION APP DESIGN

COMSOL Multiphysics delivers tools for modeling, simulation, and application design. With the Application Builder, simulation specialists can build and share simulation apps within organizations, from design and development to production and testing. See what's new in simulation technology at comsol.com/release/5.2

COMSOL, Inc.

Free Info at http://info.hotims.com/61062-789

CUSTOM RUBBER MOLDING TO EXACT SPECIFICATIONS

You probably know us best as producers of rubber molded parts. However, you may not know that we've produced many parts that other companies considered nearly impossible to make. Our specialty? Precision custom molded parts at a competitive price with on time delivery. Injection, transfer and compression molding of Silicone, Viton, Neoprene, etc. Hawthorne Rubber Manufacturing Corp., 35 Fourth Ave., Hawthorne, NJ 07506; Tel: 973-427-3337, Fax: 800-643-2580, www.HawthorneRubber.com

Hawthorne Rubber

Free Info at http://info.hotims.com/61062-790

LOW OUTGASSING SILICONE SYSTEM

Master Bond MasterSil 972TC-LO is capable of transferring heat while retaining superior dielectric properties. It bonds well to a wide variety of substrates, including metals, composites, glass, ceramics as well as many types of rubber and plastics. The system has very good flexibility and elongation. http://www.masterbond.com/tds/mastersil-972tc-lo

Master Bond

Free Info at http://info.hotims.com/61062-791

Become an INSIDER

Start your free subscription to Tech Briefs' INSIDER e-mail newsletter to keep pace with the latest technology advances and licensing opportunities in aerospace, electronics, photonics, manufacturing, and other key fields.

www.techbriefs.com/insider

HOW ACCURATE IS YOUR TORQUE MEASUREMENT?

- Our accuracy holds under field conditions that can vary
- Our MCRT® Bearingless Digital Torquemeters offer the highest overrange and overload of any similar products
- They're simple to install and tolerant of rotor-to-stator misalignments.

Our calibration laboratory is ISO 17025 accredited by NVLAP (Lab Code 200487-0) Contact: 800.632.7873 or sales@himmelstein.com http://www.himmelstein.com

S. Himmelstein and Company

Free Info at http://info.hotims.com/61062-792

A WORLD OF FIBER OPTIC SOLUTIONS

- T1/E1 & T3/E3 Modems, WAN
- RS-232/422/485 Modems and Multiplexers
- Profibus-DP, Modbus
- Ethernet LANs
- Video/Audio/Hubs/Repeaters
- USB Modem and Hub
- Highly shielded Ethernet, USB (Tempest Case)
- ISO-9001

http://www.sitech-bitdriver.com

S.I. Tech

Free Info at http://info.hotims.com/61062-793

AEROSPACE & DEFENSE™
TECHNOLOGY

Publisher ..... Joseph T. Pramberger
Editorial Director – TBMG ..... Linda L. Bell
Editorial Director – SAE ..... William Visnic
Editor ..... Bruce A. Bennett
Associate Editor ..... Billy Hurley
Managing Editor, Tech Briefs TV ..... Kendra Smith
Associate Editor ..... Ryan Gehm
Production Manager ..... Adam Santiago
Assistant Production Manager ..... Kevin Coltrinari
Creative Director ..... Lois Erlacher
Senior Designer ..... Ayinde Frederick
Global Field Sales Manager ..... Marcie L. Hineman
Marketing Director ..... Debora Rothwell
Marketing Communications Manager ..... Monica Bond
Digital Marketing Coordinator ..... Kaitlyn Sommer
Audience Development Director ..... Marilyn Samuelsen
Audience Development Coordinator ..... Stacey Nelson
Subscription Changes/Cancellations ..... nasa@omeda.com

TECH BRIEFS MEDIA GROUP, AN SAE INTERNATIONAL COMPANY
261 Fifth Avenue, Suite 1901, New York, NY 10016
(212) 490-3999 FAX (646) 829-0800

Chief Executive Officer ..... Domenic A. Mucchetti
Executive Vice-President ..... Luke Schnirring
Technology Director ..... Oliver Rockwell
Systems Administrator ..... Vlad Gladoun
Web Developer ..... Karina Carter
Digital Media Manager ..... Peter Bonavita
Digital Media Assistants ..... Peter Weiland, Anel Guerrero, Maria Sevilla
Digital Media Audience Coordinator ..... Jamil Barrett
Credit/Collection ..... Felecia Lahey
Accounting/Human Resources Manager ..... Sylvia Bonilla
Office Manager ..... Alfredo Vasquez
Receptionist ..... Elizabeth Brache-Torres

ADVERTISING ACCOUNT EXECUTIVES

MA, NH, ME, VT, RI, Eastern Canada ..... Ed Marecki
Tatiana Marshall
(401) 351-0274
CT ..... Stan Greenfield
(203) 938-2418
NJ, PA, DE ..... John Murray
(973) 409-4685
Southeast, TX ..... Ray Tompkins
(281) 313-1004
NY, OH ..... Ryan Beckman
(973) 409-4687
MI, IN, WI ..... Chris Kennedy
(847) 498-4520 ext. 3008
MN, ND, SD, IL, KY, MO, KS, IA, NE, Central Canada ..... Bob Casey
(847) 223-5225
Northwest, N. Calif., Western Canada ..... Craig Pitcher
(408) 778-0300
CO, UT, MT, WY, ID, NM ..... Tim Powers
(973) 409-4762
S. Calif., AZ, NV ..... Tom Boris
(949) 715-7779
Europe – Central & Eastern ..... Sven Anacker
49-202-27169-11
Joseph Heeg
49-621-841-5702
Europe – Western ..... Chris Shaw
44-1270-522130
Integrated Media Consultants ..... Patrick Harvey
(973) 409-4686
Angelo Danza
(973) 874-0271
Scott Williams
(973) 545-2464
Rick Rosenberg
(973) 545-2565
Todd Holtz
(973) 545-2566
Reprints ..... Rhonda Brown
(866) 879-9144, x194

Ad Index

For free product literature, enter advertisers' reader service numbers at www.techbriefs.com/rs, or visit the Web site beneath their ad in this issue.

Aerospace & Defense Technology, ISSN – 2472-2081, USPS – Application to Mail at Periodicals Postage Prices is Pending at New York, NY and additional office. is published in February, April, May, June, August, October, and December (7 issues) by Tech Briefs Media Group, an SAE International Company, 261 Fifth Avenue, Suite 1901, New York, NY 10016. Editorial, sales, production, and circulation offices at 261 Fifth Avenue, Suite 1901, New York, NY 10016. Subscription is free to qualified subscribers and Subscriptions for non-qualified subscribers in the U.S. and Puerto Rico, $75.00 for 1 year. Digital Edition: $24.00 for 1 year. Single copies $6.25. Foreign subscriptions one-year U.S. Funds $195.00. Remit by check, draft, postal, express orders or VISA, MasterCard, and American Express. Other remittances at sender's risk. Address all communications for subscriptions or circulation to NASA Tech Briefs, 261 Fifth Avenue, Suite 1901, New York, NY 10016.

POSTMASTER: Send address changes and cancellations to NASA Tech Briefs, P.O. Box 47857, Plymouth, MN 55447.

June 2016, Volume 1, Number 4

Make the Connection

Find the simple way through complex EM systems with CST STUDIO SUITE

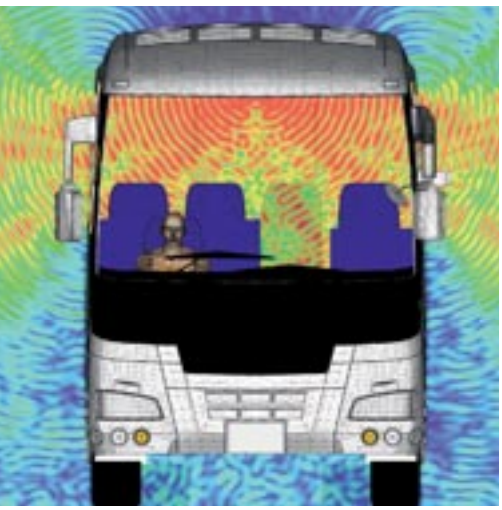

Components don't exist in electromagnetic isolation. They influence their neighbors' performance. They are affected by the enclosure or structure around them. They are susceptible to outside influences. With System Assembly and Modeling, CST STUDIO SUITE helps optimize component and system performance.

Involved in antenna development? You can read about how CST technology is used to simulate antenna performance at **www.cst.com/antenna**.

If you're more interested in filters, couplers, planar and multilayer structures, we've a wide variety of worked application examples live on our website at **www.cst.com/apps**.

Get the big picture of what's really going on. Ensure your product and components perform in the toughest of environments.

Choose CST STUDIO SUITE –
Complete Technology for 3D EM.

CST

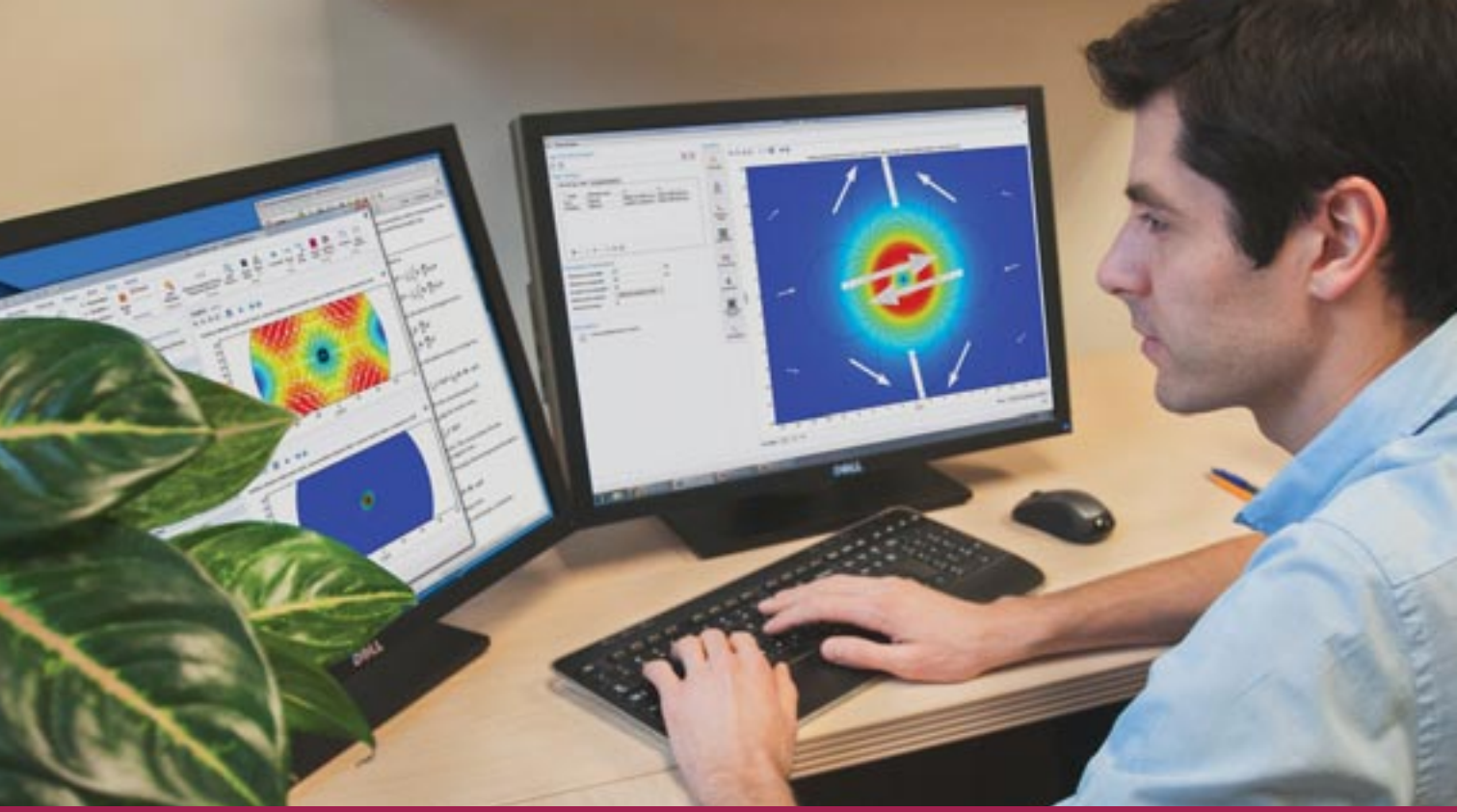

MULTIPHYSICS FOR EVERYONE

The evolution of computational tools for numerical simulation of physics-based systems has reached a major milestone.

Custom applications are now being developed by simulation specialists using the Application Builder in COMSOL Multiphysics®.

With a local installation of COMSOL Server™, applications can be deployed within an entire organization and accessed worldwide.

Make your organization truly benefit from the power of analysis.

comsol.com/application-builder

COMSOL

Free Info at http://info.hotims.com/61062-795